Multi-physics continuum modelling approaches for metal powder additive manufacturing: a review

Shekhar Srivastava and Rajiv Kumar Garg
Department of Industrial and Production Engineering, Dr BR Ambedkar National Institute of Technology, Jalandhar, India
Vishal S. Sharma
School of Mechanical, Industrial and Aeronautical Engineering, University of Witwatersrand, Johannesburg, South Africa
Noe Gaudencio Alba-Baena
Department of Industrial Engineering and Manufacturing, Universidad Autonoma de Ciudad Juarez, Juarez, Mexico
Anish Sachdeva and Ramesh Chand
Department of Industrial and Production Engineering, Dr BR Ambedkar National Institute of Technology, Jalandhar, India, and
Sehijpal Singh
Department of Mechanical Engineering, Guru Nanak Dev Engineering College, Ludhiana, India

Abstract

Purpose – This paper aims to present a systematic approach in the literature survey related to metal additive manufacturing (AM) processes and its multi-physics continuum modelling approach for its better understanding.

Design/methodology/approach – A systematic review of the literature available in the area of continuum modelling practices adopted for the powder bed fusion (PBF) AM processes for the deposition of powder layer over the substrate along with quantification of residual stress and distortion. Discrete element method (DEM) and finite element method (FEM) approaches have been reviewed for the deposition of powder layer and thermo-mechanical modelling, respectively. Further, thermo-mechanical modelling adopted for the PBF AM process have been discussed in detail with its constituents. Finally, on the basis of prediction through thermo-mechanical models and experimental validation, distortion mitigation/minimisation techniques applied in PBF AM processes have been reviewed to provide a future direction in the field.

Findings – The findings of this paper are the future directions for the implementation and modification of the continuum modelling approaches applied to PBF AM processes. On the basis of the extensive review in the domain, gaps are recommended for future work for the betterment of modelling approach.

Research limitations/implications – This paper is limited to review only the modelling approach adopted by the PBF AM processes, i.e. modelling techniques (DEM approach) used for the deposition of powder layer and macro-models at process scale for the prediction of residual stress and distortion in the component. Modelling of microstructure and grain growth has not been included in this paper.

Originality/value – This paper presents an extensive review of the FEM approach adopted for the prediction of residual stress and distortion in the PBF AM processes which sets the platform for the development of distortion mitigation techniques. An extensive review of distortion mitigation techniques has been presented in the last section of the paper, which has not been reviewed yet.

Keywords Additive manufacturing, FEM, Residual stress, Numerical modelling, Metal additive manufacturing, PBF, Rapid manufacturing, Computational model, Numerical simulation, Distortion, DEM, Powders

Paper type Literature review

Nomenclature

AM	= additive manufacturing;
SLA	= stereo-lithography;
DLP	= direct laser printing;
3DP	= 3D printing;
FDM	= fused deposition modelling;
LOM	= laminated object manufacturing;
DMLS	= direct metal laser sintering;
SLM	= selective laser melting;
EBM	= electron beam melting;
SLS	= selective laser sintering;
SHS	= selective heat sintering;
SMS	= selective mask sintering;
HSS	= high speed sintering;
SLP	= selective laser printing;
DMD	= direct metal deposition;

The current issue and full text archive of this journal is available on Emerald Insight at: **https://www.emerald.com/insight/1355-2546.htm**

Rapid Prototyping Journal
 [ISSN 1355-2546]
[DOI 10.1108/RPJ-07-2019-0189]

Received 20 August 2019
Revised 27 November 2019
Accepted 27 January 2020

LENS = laser engineered net shaping;
LC = laser consolidation;
LD = laser deposition;
IFF = ion fusion formation;
EBDM = electron beam direct melting;
SMD = shape metal deposition;
ABS = acrylonitrile butadiene styrene;
PLA = poly lactic acid;
PLGA = poly lactic-co-glycolic acid;
UV = ultra violet;
FE/FEM = finite element/ finite element method;
DEM = discrete element method;
LB = Lattice Boltzmann;
FV/FD = finite volume/finite difference;
PF = phase field;
CA = cellular automaton;
DED = direct energy deposition;
PBF = powder bed fusion;
JKR = Johnson Kandall Roberts;
RDF = radial distribution function;
SEBM = selective electron beam melting;
M-DVRT = micro differential variable reluctance transducer;
CMM = coordinate measuring machine;
MJ = material jetting; and
BJ = binder jetting.

1. Introduction

Additive manufacturing (AM) (3 D printing) is defined as the process of layer-by-layer manufacturing of a 3 D object by using its 3 D CAD model and a dedicated machine. The current and future demand and sale of metal AM technologies for different geographical locations are shown in Figure 1(a), which shows a forecasting demand in 2017 and 2022 respectively in around the globe and annual growth is compared for the five-year term of 2007 to 2012 and 2012 to 2017 (Bikas *et al.*, 2016). A growth in sale [Figure 1(b)] of approximately 80 per cent (983 units of metal AM machines sold in 2016 to 1768 units sold in 2017) due to respective development and commercialisation as given by *Wohler's Report 2018*, is putting pressure on established producers of AM systems (Wohlers Associates, 2018; Wohlers and Gornet, 2012), whereas it is realistic to forecast an excess of $7.5 billion in the AM domain by 2020 based on the growth and continual deployment of today's technology (AM Special Interest Group, 2012; Wohlers, 2016).

AM gains huge popularity in the field of manufacturing engineering and systems in the past two decades because of the development of various AM processes and novel materials in aerospace, biomedical and other industries (Leigh *et al.*, 2012). While present AM machines are remarkably improved with respect to the earlier machines, defects such as residual stresses and thermal gradients and material supply issues, still

Figure 1 (a) Worldwide demand of AM Machines – Summary and (b) A rise in metal AM machine sale

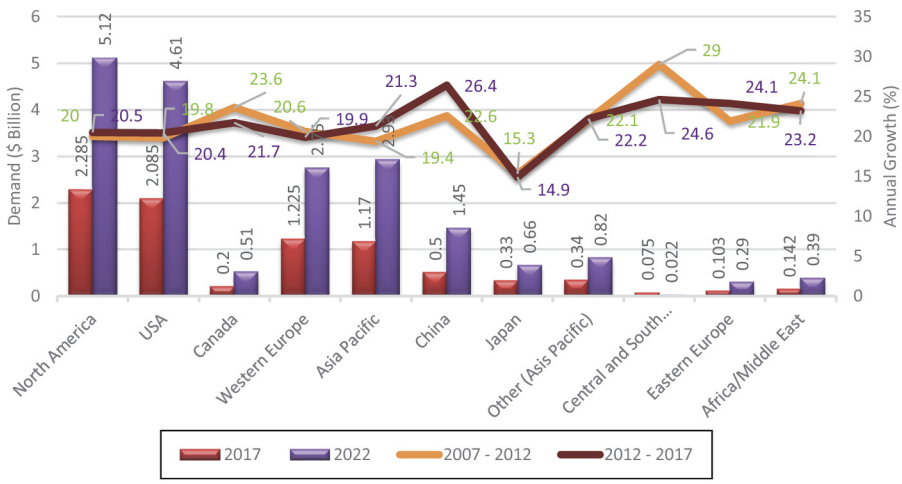

(a)

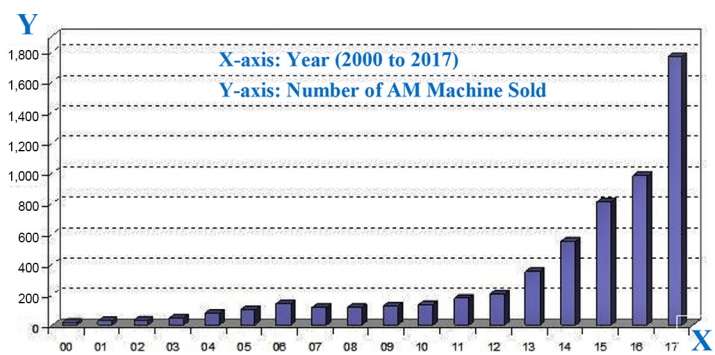

(b)

exist in this technology as stated by early researchers (Srivatsan and Sudarshan, 2016; Gibson *et al.*, 2009). These defects occurred while processing components through AM is a peculiar concern for a successful application.

2. Types of additive manufacturing processes

AM is defined in the ASTM-F2792 standard as "the process of joining materials to make objects from 3 D model data, usually layer upon layer, as opposed to subtractive manufacturing technologies" (ASTM Standard, 2012; AM Special Interest Group, 2012). The important criteria for the selection of an AM machine are its speed, cost of the component, the variability of materials and its colour capabilities (Boley *et al.*, 2015; Rubenchik *et al.*, 2015; Pham and Dimov, 2001; Turner *et al.*, 2014). The following sub-sections describe the variants of AM processes as per the standard classification given in ASTM/ISO 52900:2015 (Umaras and Tsuzuki, 2017) along-with a feedstock-based classification (Figure 2) of metal-AM.

Figure 2 Classification of metal AM based on the feed stock materials

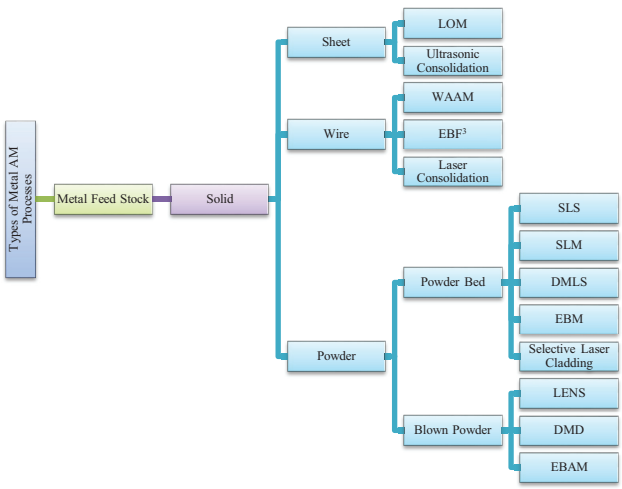

2.1 Material extrusion

The material extrusion (ME) process uses a heating nozzle for softening/melting of material to deposit and form the geometry as per its CAD as Figure 3(a). Fused deposition modelling (FDM) (Bikas *et al.*, 2016; Chryssolouris, 2015; Raju *et al.*, 2018) and robocasting (Cesarano, 1999; Cesarano *et al.*, 1997; Guo and Leu, 2013), fused filament fabrication and fused layer modelling are the types of ME process in which FDM uses polymer wire to print parts in aerospace and biomedical prototyping and automotive industries (Ingole *et al.*, 2009; Ivanova *et al.*, 2013).

2.2 Material jetting

Material jetting (MJ) method was first introduced in the 1980s with patent related to the development of ballistic particle manufacturing, which uses a drop on demand deposition of materials on a substrate (Additive3d., 2020). Liquid photo-polymers are fed as a jet spray in a controlled manner as per the design of components [Figure 3(b)]. 3DP (Bose *et al.*, 2013; Kruth *et al.*, 1998; Guo and Leu, 2013), ink-jet printing (IJP) (Le, 1998), multi-jet modelling (Chua *et al.*, 2010; Wohlers, 2016; Bourell *et al.*, 2001) and ballistic particle manufacturing (Wohlers, 1991; Dahotre and Harimkar, 2008) are types of MJ process in which IJP is widely used in electronics industries for printing complex electronic circuits (Sirringhaus *et al.*, 2000).

2.3 Binder jetting

Binder jetting (BJ) process is one the multistep AM process originally developed at Massachusetts Institute of Technology, USA in the early 1990s (Meteyer *et al.*, 2014) and commercially adopted in 2010 (Sachs *et al.*, 1990). This process can be fed with metals/alloys (Al alloys, iron-based, Ni & Co- based, etc.) and ceramics (glass, graphite, etc.) for the printing of components. The BJ process [Figure 4(a)] mainly consists of two types of materials, i.e. build material as metal alloy or ceramic whereas binder material is used to glue the build materials.

2.4 Sheet lamination

The components of this AM category include an adhesive applied paper/plastic, a cutter (usually a laser) and a roller. The film is then pressed down on the previous layer and by a heated

Figure 3 Principle and Schematic (a) ME (Bikas *et al.*, 2016) and (b) MJ (Groth *et al.*, 2014)

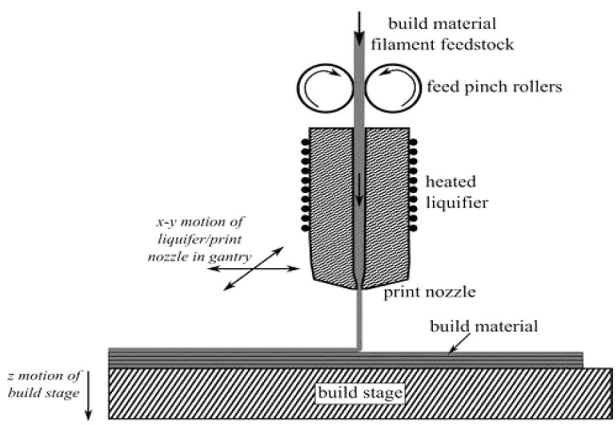

(a)

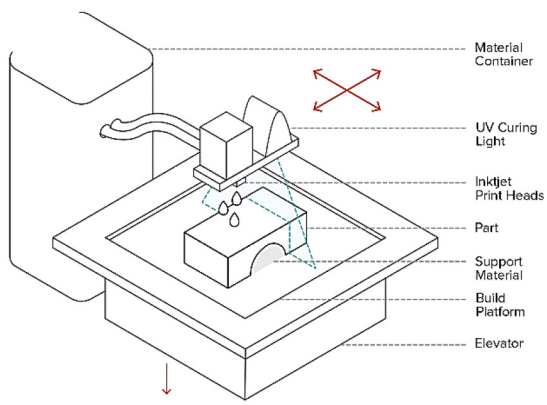

(b)

Figure 4 Principle and schematic

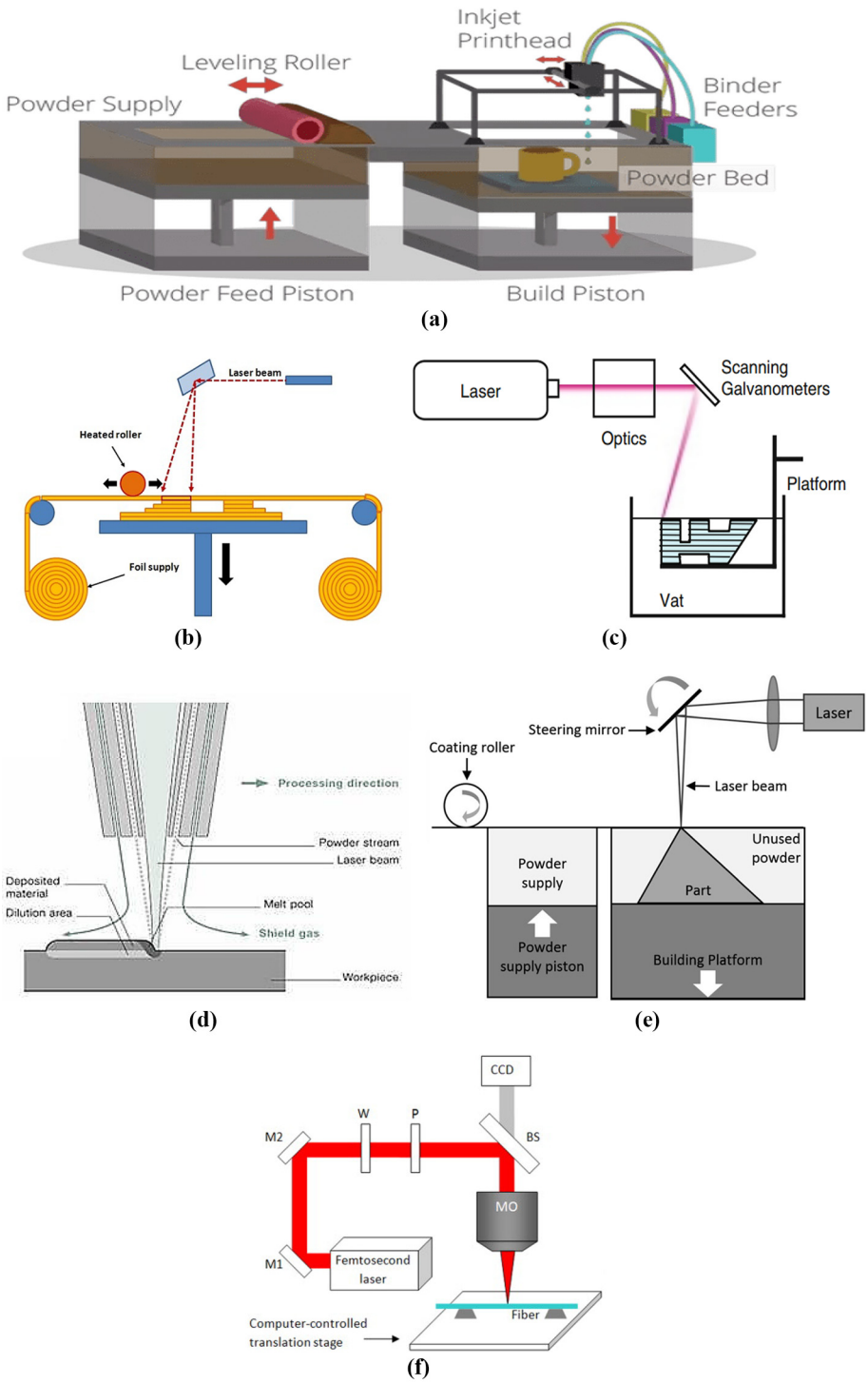

Notes: (a) Binder Jetting (Chen *et al*., 2016); (b) Sheet Lamination (Bikas *et al*., 2016); (c) Vat Polymerization (Bikas *et al*., 2016); (d) DED AM (Bikas *et al*., 2016); (e) PBF AM (Source: Virtual Prototyping & Bio-Manufacturing in Medical Applications, Merlin Projects) (f) Laser DW (Wang *et al*., 2015)
Source: Laser Surface Engineering, Woodhead Publishing, 2015

roller which in turn activates the adhesives present on the downward face of the paper to bind the papers. A schematic for such processes is shown in Figure 4(b). LOM (Pham and Gault, 1998) and SFP (Dahotre and Harimkar, 2008; Corbel *et al.*, 1994) are two types of sheet lamination AM process which are very limited in use.

2.5 Vat polymerisation

Vat polymerisation uses the concept of phase change in its processing i.e. based on the same material phase change properties, in which a photosensitive polymer resin is exposed to a low-power laser. Laser polymerisation is used for polymers resins having low strength therefore, used in the field of prototyping and non-structural applications (Pham and Gault, 1998; Corbel *et al.*, 1994; 3D Systems, 2018; Zhang *et al.*, 2002; Singh *et al.*, 2012). Stereo-lithography, direct laser printing, continuous liquid interface production by Carbon and daylight polymer printing by Photocentric are the variants of vat polymerisation [Figure 4(c)] (3dexperience, 2019).

2.6 Direct write

Direct write (DW) AM technologies enable the selective deposition and patterning of liquid feedstock onto the substrate which extends its application in the field of embedded electronics. DW technologies have been developed for 2 D writing but some DW processes are now used for the production of high-resolution 3 D components i.e. laser chemical vapour deposition (LCVD), focussed ion beam DW, aerosol jet process, laser induced forward transfer (LIFT), matrix-assisted pulsed-laser DW (MAPLE), and nozzle dispensing processes (Gibson *et al.*, 2009; Vaezi *et al.*, 2013). DW assembly deposits inks at room temperature with controlled printing speed and pressure which depends on inks rheology and nozzle diameter (Perez and Williams, 2013). A schematic working of femtosecond laser direct writing of optical fibre is shown in Figure 4(f).

2.7 Directed energy deposition

The directed energy deposition (DED) AM processes consist of metal feedstock in the form of the powder (blown through a concentric nozzle into a molten pool) and wire [Figure 4(d)]. Therefore, power source (laser, electron beam or plasma arc) and material (wire or blown powder) follow the path of deposition provided through the CAD model (Baykasoglu *et al.*, 2018; Heigel *et al.*, 2015). Laser engineered net shaping (LENS) process is one of the blown powder DED AM processes, mostly used for a significant precision process like turbine blades repair. Apart from blown powder DED, wire arc AM (Graf *et al.*, 2018) and electron beam freeform fabrication (EBF^3) (Chen *et al.*, 2018) is the variant of the DED AM process.

2.8 Powder bed fusion

Powder bed fusion (PBF) AM process uses a medium to low-power laser source to melt the powder feedstock. A laser source is used to selectively melt the powder bed and after cooling produces the final component [Figure 4(e)]. Metal AM processes and their characteristics are given in Table I. Another variant of the PBF AM process is Electron Beam Melting (EBM). A high voltage (30-60 kV) (Bikas *et al.*, 2016; Woesz, 2010; Shellabear and Nyrhila, 2004) electron beam melts the metal powder in a vacuum chamber to avoid oxidation.

3. Industrial need of modelling

AM is not only the state-of-the-art technology that has the capability to replace many conventional and non-conventional manufacturing techniques, but also a remarkable manufacturing technique allowing new business domains, new materials and products and supply chain to grow. Modelling and simulation will play a judgemental role in the modification of conventional trial and error approach for selection of process parameters and quantify the influence of it on various mechanical properties with an understanding of the basic the physical phenomenon. To improve the acceptance criteria as per underlying physical phenomena which evident themselves in the as-built material properties, challenges range from the market value consideration (limited build speed and sizes) to technical compatibility (residual stresses and distortion) in the process has to be considered carefully. In metal AM processes, distortion (Withers and Bhadeshia, 2001; Mercelis and Kruth, 2006), due to residual stresses while solidification, is one of the major concerns. To minimise distortion, the appropriate mode of distortion should be identified as discussed in Mashubuchi (1980), Kula and Weiss (1982) and its effect should be mitigated before application.

Mukherjee *et al.* (2017a) mentioned that a quantitative explanation of the involvement of AM process variables on thermal distortion and a practical approach to diminish the effect of distortion is scarce. From the manufacturing point of view of end product or assemblies, optimisation of process parameters of any manufacturing process is a must. To serve this purpose in metal AM, in-depth knowledge of the process itself is required. Such an understanding of the process can be attained by either experimentation to form an empirical relation between input and output parameters or by understanding the basic physical phenomena. To address such challenges in AM components, computational modelling has an important role to play when it is compared with other manufacturing processes.

4. Review of modelling approaches

Metal AM processes have been facing a lot of challenges since its introduction in terms of the quality of components produced. These challenges are the conceptualisation of defects remedies and its mitigation during fabrication or post fabrication. There are various defects occurring due to various processing conditions in AM components i.e. keyhole defect (Teng *et al.*, 2017; Kroos *et al.*, 1993; Cao *et al.*, 2007) [Figure 5(a)], layer bonding (Markl and Körner, 2016; Rausch *et al.*, 2018), channels (Bauereiß *et al.*, 2014; Rausch *et al.*, 2018), porosity (Markl and Körner, 2016; Bauereiß *et al.*, 2014; Vandenbroucke and Kruth, 2007) [Figure 5(b)], lack of fusion (Sames *et al.*, 2014; Mukherjee *et al.*, 2016; Darvish *et al.*, 2016), cracking (Mukherjee *et al.*, 2017b; Carter *et al.*, 2012; Zaeh and Kahnert, 2009) [Figure 5(c)], and dimensional accuracy (Frazier, 2014; Mukherjee *et al.*, 2016), loss of alloying elements (Mukherjee *et al.*, 2017a; Brice *et al.*, 2009), poor surface quality (Heigemann *et al.*, 2016; Strano *et al.*, 2012; Rahmati and Vahabli, 2015; Niu and Chang, 1999; Gu and Shen, 2009) (Figure 7). These defects are the major setback for AM processes to be adopted worldwide in its application fields. To counter these defects, various researchers across the world, are adopting analytical and numerical

Table I Current trends/application – laser-based AM processes

AM process	Materials	Power source	Current trends/applications
Selective Laser Sintering (SLS) [Patent-1989]	Metal Powders, Polymers and Composites, Polymer coated Ceramics (Tolochko *et al.*, 2000; Boley and Rubenchik, 2013)	Laser Beam (From 7 – 10 W for plastics to 50-200 W for metals and ceramics) (Singh *et al.*, 2012; Sachdeva *et al.*, 2013; Beaman *et al.*, 1996; Singh *et al.*, 2013; Sharma *et al.*, 2015)	Biomedical Implant Fabrication and Drug Delivery Development of biomedical models and scaffolds (Mainprize *et al.*, 2018; Fina *et al.*, 2018)
Selective Laser Melting (SLM) [Patent-1995]	Cu, Tool Steel, Co-Cr, Ti, W, Al, SS, Au (Yadroitsev, 2009; Abe *et al.*, 2011)	High-powered (200-2000 W) Yb-fiber optic laser (Hänninen, 2001; Yang *et al.*, 2010; Buchbinder *et al.*, 2011)	Novel Mg-based alloys by SLM for biomedical applications (Long *et al.*, 2018)
Direct Metal Laser Sintering (DMLS) [Patent-1994]	Ti6Al4V, IN625 and 718, 17-4 PH, SS 316 L, AlSi10Mg, CrCoMo (Stratasysdirect, 2018; Shishkovsky *et al.*, 2007; Yadroitsev *et al.*, 2007)	200 W Yb fibre laser (Syvänen *et al.*, 2005)	Electronics Industry
LENS [Patent-1997]	CP-Ti, Ti6Al4V, IN625, IN718, IN690, SS 316 L, PH 17-4, TiC, WC, CrCo (Bikas *et al.*, 2016; optomec, 2020)	Nd – YAG High Power Laser (3 kW – 4 kW) (optomec, 2020)	Nanotechnology and Electronics (Liu *et al.*, 2018; Jay *et al.*, 2018) Material Development and Properties Modification
Laser Powder Deposition	CP-Ti, Ti6Al4V, IN625, IN718, IN690, SS 316 L, PH 17-4 (Vilar, 2014; Woesz, 2010)	2 kW CO_2 Laser (Vilar, 2014)	Materials Development (Tiwari *et al.*, 2018; Hui *et al.*, 2018) Strengthening mechanism of AlSi10Mg using DMLS (Hadadzadeh *et al.*, 2018)
Selective Laser Cladding	Fe, Cr and Ni (Soares and Perez-Amor, 1987; Jeng *et al.*, 2000)	1.5W CO_2 Laser (Jeng *et al.*, 2000)	Multi-Material Structures Inconel 718 and Cu bimetallic structure (Onuike *et al.*, 2018) Ti-Al_2O_3 multi material structure (Zhang and Bandyopadhyay, 2018) Shape Memory Alloys Microstructure and properties of LENS prepared Ni-Ti alloys (Baran and Polanski, 2018) Ultrasonic assisted LENS Microstructure and mechanical characterisation of Inconel 718 (Ning *et al.*, 2018) Hybrid Processes (Sealy *et al.*, 2018)

Figure 5 (a) Keyhole formation, (b) porosity occurred in AM Part (Source: 8th International Symposium on Super-alloys 718 and Derivatives) (Sames *et al.*, 2014) and (c) Layer Delamination and Cracking in AM parts (Source: Annual International Solid Freeform Fabrication Symposium 2013) (Kempen *et al.*, 2013)

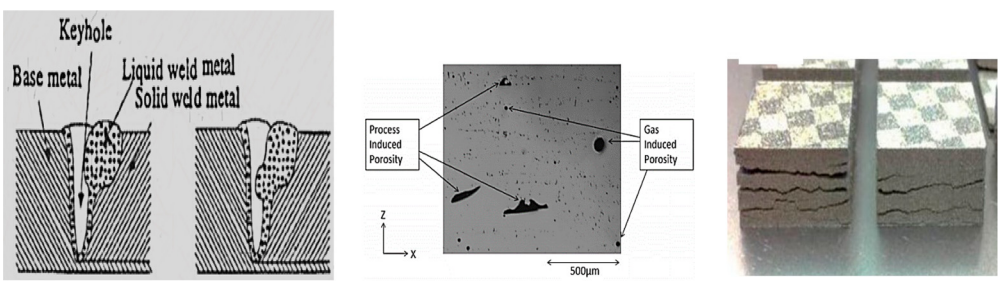

(a) (b) (c)

modelling approaches for a better physical understanding of the process at multi scale level. Some of the numerical modelling approaches are listed in Table II with its relevant fields to provide better understanding at various scale for AM processes i.e. discrete element method (DEM) approach demonstrates the production of realistic powder bed with appropriate size segregation and packing distribution by considering particle shape, cohesion between particles, stiffness of particles, nature of contact, damping. Whereas, process and performance modelling can be achieved using finite element method (FEM) which demonstrates the modelling of the melting and solidification process and quantification of residual stress by evaluating the amount of continuous heat addition and losses over deposition. Further, the application of the Lattice Boltzman (LB) method in AM demonstrate the simulation of thermal transport of fluids with free surfaces and a solid liquid

Table II Numerical modelling approaches and its application in AM

Application area in AM	Numerical methods	Reason/origin	Ref.
Material Supply/Powder Bed Generation	DEM	Surface roughness and porosity of layer due to geometric properties depends on coating process (Parteli and Pöschel, 2016)	Markl and Körner (2018), Johanson (2016), Cundall and Strack (1979)
Heat Addition (Melting and Solidification), Hydrodynamics and Elastoplastic Modelling	Finite Element (FE) Method; Lattice Boltzmann (LB) Method; FV Method; Finite Difference (FD) Method	Residual stresses/distortion is a common defect in metal AM due to contraction of layer (Nickel *et al.*, 2001) and non-homogeneous thermal cycles (Venuvinod and Ma, 2004)	Khairallah and Anderson (2014), Denlinger *et al.* (2014a), Dai and Gu (2013), Chen and Zhang (2004), Taylor *et al.* (2002), Schoinochoritis *et al.* (2014)
Microstructure and Grain Structure Evolution	PF Modelling; CA Method; Monte Carlo Approach	Control of microstructure and grain growth and structure in metal AM results in control of various defects stated above in Section 4	Anderson *et al.* (2000), Sahoo and Chou (2015), Baykasoglu *et al.* (2018), Lu *et al.* (2017), Rai *et al.* (2016), Zhang *et al.* (2016), Srolovitz *et al.* (1684), Rappaz and Gandin (1993)

phase transformation (Attar and Körner, 2011). Finite volume (FV) method is a specialised FE method serves the same explanation by demonstrating the conservation laws over a boundary of arbitrary volume by an integral formulation (Eymard *et al.*, 2000). For the modelling of microstructure and grain growth, Phase field (PF) models demonstrate the interaction of interface between two adjoining phases to have a non-zero width. An additional variable named PF which characterise the phase of material at any spatial and temporal coordinates (Wheeler *et al.*, 1996). Cellular automaton (CA) method provides automaton (CA) method provides an algorithm to characterise the discrete temporal and spatial microstructure evolution by using the network of regular cells (Raabe, 2002). Monte Carlo simulations, which had been developed by Anderson *et al.* (1984) for examining grain growth, demonstrate the minimisation of interfacial energy by considering the energies of sites lying in different grains.

4.1 Modelling of material addition

PBF process includes a heat source as a laser or electron beam in which material supplied is in the form of a powder bed before it is exposed to the heat source. Since the supply of material is in the form of powder, the first challenge is to model the material supply along with a moving heat source. As this article focuses on the PBF AM process, therefore this section will discuss the Rain-Drop modelling and DEM approaches adopted for powder layer deposition modelling.

4.1.1 Rain-drop modelling

In the rain-drop models, positions of each individual particle are analytically computed by neglecting the particle distribution process and by describing the powder particle packing density (Jullien and Meakin, 1987; Meakin and Jullien, 1987). The first contact with all formerly settled particles is calculated by a vertical trajectory as soon as the random horizontal position has been chosen for each particle. Afterward, the particle is allowed to rotate to the next contacts until the minimum potential energy is reached. Rain-drop models are effectively applied for 2 D and 3 D simulations (Zhou *et al.*, 2009; Körner *et al.*, 2011). However, the final relative density of the particle packing is too high to be adjustable in the model for the PBF AM process and the values between 40 per cent to 60 per cent are recommended (Bauereiß *et al.*, 2014; Markl and Körner, 2018; Venuvinod and Ma, 2004). Körner *et al.* (2011) stated that adopting the method of deleting a single particle after layer generation can be a solution to achieve the desired packing density. This modelling approach creates defects in the powder layer as mentioned above, which further affects the final porosity and also forms the multi-layer channel in the components made through the PBF AM process. Due to defects produced, this modelling approach is not very famous to be applied in PBF AM powder layer deposition (Bauereiß *et al.*, 2014; Rausch *et al.*, 2018). Alternatively, the DEM approach has been considered for the deposition of a layer in the PBF AM process, discussed in the next section.

4.1.2 Discrete element method

DEM is used for the modelling of a powder bed formation in which all powder particles are considered simultaneously in the analysis (Markl and Körner, 2018). A procedure for the formation of a powder bed can be seen in Figure 6 in which a roller is to roll down a pile of metal powder into an organised layer of a certain thickness. Cundall and Strack (1979) introduced the DEM simulations initially for describing the mechanical behaviour of assemblies of discs and spheres. This mesoscale modelling is used to understand the particle-based properties at the individual particle scale and powder spreading process parameters like the speed of roller, shape and size of roller, shape and size of granules etc., on uniformity and smoothness of pre heated powder bed i.e. spatial distribution of powder bed, bed porosity and thickness. Further, Johanson (2016) developed a rolling theory for granular solids on the basis of plain strain deformation of an isostatic, frictional, cohesive and compressible solid. The theory gives a procedure to find the values of roll force, roll torque, roll diameter, the roll

Figure 6 Powder layer deposition with a roller (a) before and (b) roller in action

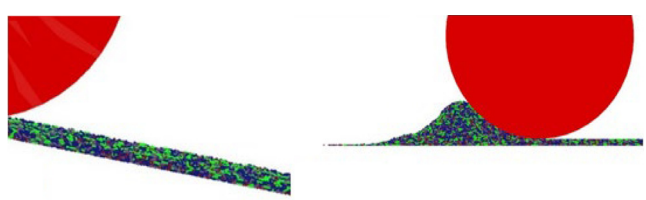

(a) (b)

gap, and the feed pressure required to cause maximum pressure to be applied on the solid. In continuation, Zok *et al.* (1991) developed a model for particle packing (packing density) in a binary composite system which infers that the packing efficiency defined by the ratio of packing density to the ideal packing density is controlled by the particle to inclusion size ratio. However, in this context, a review article (Lange *et al.*, 1989) published on two issues i.e. packing powder system and constrained densification of powder particles for the preparation of ceramic composite which can be referred for more details about DEM approach. Additionally, Monte Carlo simulation (Cao *et al.*, 2007) is also used for the random packing of unequal shaped and sized particles in which particles obeys a log-normal distribution having a probability density function given in *equation (iii)* with radius of particle as "*r*". Karapatis *et al.* (1999) in their work shown that overall quality of SLSed part depends on the density of the powder layer placed before sintering process with a conclusive increase in density from 53 per cent to 63 per cent when 30 per cent of the fine powder is added to a coarse powder with a coarse-to-fine ratio of 1:10. Shanjani and Toyserkani (2008) performed 1 D slab analysis of counter rotating roller compaction of powder and showed that there is a difference of minimum 7.6 per cent and a maximum of 11 per cent in the final densities with spherical and dendritic shaped copper powders. Apart from the proposed modelling given in Cundall and Strack (1979), some researchers modified the application in the field of powder layer deposition in PBF AM process, few prominent results are given in Table III for better understanding of the DEM approach applied to PBF process which in turn deposited effective layers and yielded better material properties of the component produced. The delivery of powder particles on the substrate of PBF AM process generally depends on various powder properties like particle size distribution, the shape of the particle and flowability (Markl and Körner, 2018). Some of the other physical phenomena considered in the simulation of powder particles are explained in Herbold *et al.* (2015), i.e. cohesion and stiffness of particles. As explained above DEM approach is a Lagrangian approach in which the modelled zones consider the point inside their own point of reference. DEM approach uses Newton's law of motion for the conservation of linear as well as angular momentum which is given in the following equations (Mindt *et al.*, 2016).

$$m_i \frac{dv_i}{dt} = \sum_j f_{ij} + f_b^i + m_i g \tag{1}$$

$$I_i \frac{dw_i}{dt} = \sum_j m_{ij} + m_i^b \tag{2}$$

Despite the fact has been established that the quality of the powder is a key factor for the final acceptance of the part produced through metal AM processes (Slotwinski *et al.*, 2014; Sutton *et al.*, 2016), a powder-based study should be conducted to investigate the effect of particle geometry and size on final part distortion and residual stresses (Figures 6-8).

$$f(r) = \frac{1}{\sqrt{2\pi}.\sigma r} e^{\frac{-(\ln r - \ln r_0)^2}{2\sigma^2}} \tag{3}$$

4.2 Thermo-mechanical modelling

When a part is produced through metal AM process, the material experiences spatial heating, melting, solidification and cooling of the entire part. Due to this, permanent deformation and dimensional instability occur in the part depending upon the thermo-physical properties, rigidity of materials, transient thermal fields and selected process parameters (Venuvinod and Ma, 2004). The physical mechanism that controls the PBF AM processes and exhibits complex working conditions are very similar to laser or electron beam welding processes (Wen and

Table III Discrete element modelling approaches for AM

Author	Year	Process	Methodology	Results
Deng and Davè (2013)	2013	A multi sphere JKR model is coupled with DEM approach	EDEM2.4 software and JKR Model is used for simulations of particles	The surface energy and aspect ratio have a significant effect on porosity and packing structure
Zohdi (2014)	2014	Particle movement due to surface contact and particle-particle contact is examined	A customised DEM algorithm is used for the simulation of powder particle dynamics	Framework model suggested handles depositions with different particle sizes and particles with binders
Parteli and Pöschel (2016)	2016	A numerical tool has been developed for deposition through a roller	An open source library LIGGGHTS for DEM simulations	Blade speed and size distribution affect the surface roughness and packing porosity
Haeri *et al.* (2017)	2017	DEM approach to explore the effect of particle shape on various outputs	The LAMMPS code is used for DEM simulations	Bed quality depends on aspect ratio and blade velocity. Roller leads blade spreader in terms of the quality of the formed bed
Kempen *et al.* (2013)	2017	Powder bed formed due to DEM approach and as per BCC structure has been compared	The powder scale model using DEM technique is applied to the raking process	Powder particle spreading and packing controls the melt pool size and segregation of particles leading to a different powder size distribution
Markl and Körner (2018)	2018	A stochastic algorithm is adopted to form an erratic powder bed	A classical DEM coupled with a grid-based solver is used	The model provides a physical relative density and an appropriate powder particle size distribution

Figure 7 A melt morphology showing balling effect

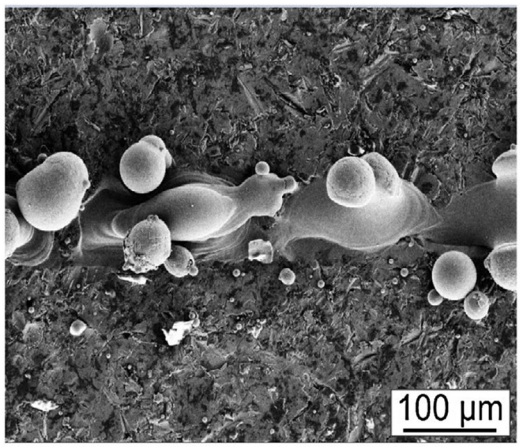

Source: Löber *et al*. (2014)

Figure 8 Heat transfer modes in laser-based AM

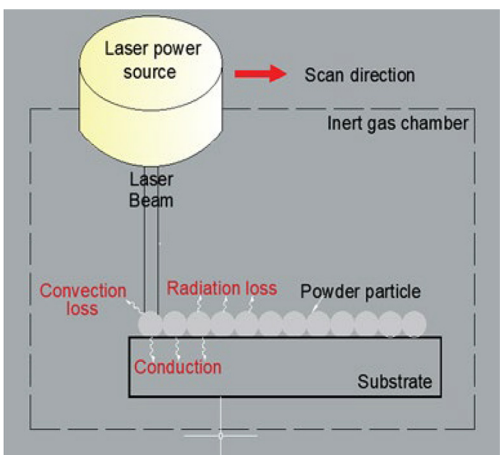

Shin, 2010). Modelling of defects like residual stress and distortion in the parts produced by welding has been the active research area for the researchers, industrialists and academicians across the globe since early 1970s (Masubuchi, 1970; Hibbitt and Marcal, 1973; Andersson, 1978). In 1980s, numerical models in these references (Argyris *et al.*, 1982; Papazoglou and Masubuchi, 1982), development of "double ellipsoidal" heat input model by Goldak *et al.* (1984), models for phase transformation in weld zones (Leblond and Devaux, 1984; Watt *et al.*, 1988; Henwood *et al.*, 1988), provided a significant improvement towards the challenges occurred due to distortion in welded components. Since the models described above are the domain of 2 D modelling, 1990s and 2000s witnessed the development of 3 D modelling for various welding processes (Tekriwal and Mazumdar, 1988; Karlsson and Josefson, 1990; Tekriwal and Mazumdar, 1991; Brown and Song, 1992) like the prediction of thermal stresses and distortion (Michaleris and De-Biccari, 1997; Michaleris *et al.*, 2006; Zhang *et al.*, 2007) to its minimisation and mitigation (Michaleris and Sun, 1997; Michaleris *et al.*, 1999).

Since welding and metal AM processes share the same experience of heat addition, melting and solidification therefore modelling techniques, which were earlier used to understand the welding process, had been extended to model metal AM processes. To model the metal AM process, there is an important challenge to develop a model that can be able to provide information at overall scale of the component. Residual stress and distortion which can cause the failure of the component while in application due to fatigue, are the domain of interest at the overall part scale. Since there are almost kilometres of heat source interpolation and more than thousands of powder layer deposition in a single component fabrication. Thus, imposing a significant computation challenge for the person involved in it. Therefore, a computational model required which takes lesser time without losing the sufficient support of fundamental physical phenomena involved, can be integrated with automated process optimisation. Thermo-mechanical models, although neglect the details of laser-powder particle interaction but are able to provide part level details, i.e. residual stress and distortion, both during and after the component is produced (Francois *et al.*, 2017). The computational challenge while performing thermomechanical modelling of PBF AM processes are the dissimilar spatial and temporal scales of localised heating with respect to the overall heating and actual time of fabrication which is considerably hours and often days. The following sections will describe thermo-mechanical modelling and its components in detail whereas Figure 9 shows a flow-chart for the thermo-mechanical modelling approach used for PBF AM processes.

4.2.1 Modelling of heat transfer and fluid flow

To numerically model the metal AM process, governing equations of mass, momentum and energy conservation are needed as given in Table IV. In the above equations, subscript s and l represents a solid and liquid phase in the melt pool respectively whereas t, μ and T are the time, dynamic viscosity and temperature respectively. Several other inputs to these equations are continuum density ρ, vector velocity V, enthalpy "h", and thermal conductivity "k" defined in (Fan and Liou, 2012). Additionally, there is a requirement of thermo-physical properties and appropriate boundary conditions discussed in later sections. Some of the early approaches of thermo-mechanical modelling of a single metal droplet and substrate interaction using FEM packages to provide a basis for further challenges are given in Ref. (Trapaga et al, 1992; Chin *et al.*, 1996a, 1996b; Klingbeil *et al.*, 1998; Cervera and Lombera, 1999; Dai and Shaw, 2001; Fan and Liou, 2012; He *et al.*, 2003, 2004; Raghavan *et al.*, 2013). In that context, the phase transformation effect has been studied recently by Bartel *et al.* (2019) using shape memory alloys in the fully coupled thermo-mechanical model. A constitutive model has been developed to accurately determine the process induced eigenstresses on the basis of energy density and energy minimisation in general and specific consideration of multiple solid phases of used material. However, basically to quantify the residual stress and distortion in the component due to heat transfer, Fourier's law of heat conduction is needed considering a continuum in the system:

Figure 9 Thermo-mechanical modelling flowchart

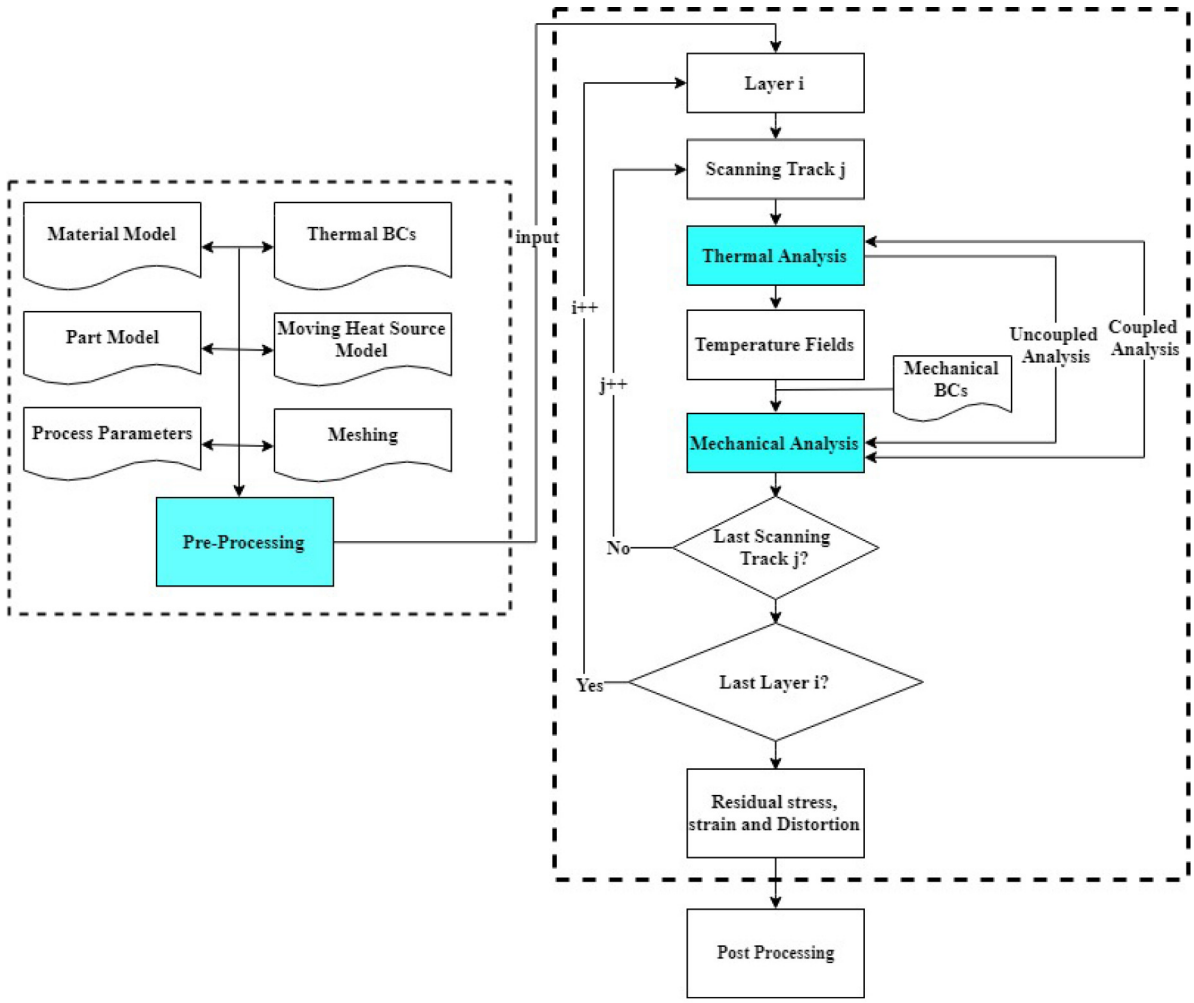

Source: Luo and Zhao (2018)

Table IV Governing equations for mass, momentum and energy balance in AM

Physical phenomena	Governing equations	Ref.
Mass Transfer	$\frac{\partial \rho}{\partial t} + \nabla \cdot (\rho V) = 0$	Fan and Liou (2012)
Momentum Conservation	$\frac{\partial}{\partial t}(\rho u) + \nabla \cdot (\rho V u) = \nabla \cdot \left(\mu_1 \frac{\rho}{\rho_l} \nabla u\right) - \frac{\partial p}{\partial x} - \frac{\mu_l}{K_x}\frac{\rho}{\rho_l}(u - u_s) + \rho g_x[1 - \alpha(T - T_0)] + F_{Sx}$	Fan and Liou (2012)
	$\frac{\partial}{\partial t}(\rho v) + \nabla \cdot (\rho V v) = \nabla \cdot \left(\mu_1 \frac{\rho}{\rho_l} \nabla v\right) - \frac{\partial p}{\partial y} - \frac{\mu_l}{K_y}\frac{\rho}{\rho_l}(v - v_s) + \rho g_y[1 - \alpha(T - T_0)] + F_{Sy}$	
Energy Balance Equation	$\frac{\partial}{\partial t}(\rho h) + \nabla \cdot (\rho V h) = \nabla \cdot (k \nabla T) - \nabla \cdot [\rho(h_l - h)(V - V_s)] + S$	Fan and Liou (2012)

$$\frac{\partial}{\partial x}\left(k\frac{\partial T}{\partial x}\right) + \frac{\partial}{\partial y}\left(k\frac{\partial T}{\partial y}\right) + \frac{\partial}{\partial z}\left(k\frac{\partial T}{\partial z}\right) + \dot{q} = \rho C_p \frac{\partial T}{\partial t} \tag{4}$$

where k is thermal conductivity, T is the continuum temperature, ρ is the density, Cp is the specific heat, $\dot{q}$ is the rate of heat input to the system, and t is the time of interaction of laser and powder layer. Solid-liquid-solid transformation in the heat addition process is being captured by introducing change in enthalpy in the Fourier's law of heat conduction. Therefore, the above equation is modified as:

$$\frac{\partial}{\partial x}\left(k\frac{\partial T}{\partial x}\right)+\frac{\partial}{\partial y}\left(k\frac{\partial T}{\partial y}\right)+\frac{\partial}{\partial z}\left(k\frac{\partial T}{\partial z}\right)+\dot{q}=\rho\frac{\partial H}{\partial t} \tag{5}$$

Considering initial temperature of the system as ambient temperature (T_a), the heat flux added to the molten pool and the losses from the free surface of the system due to convection and radiation, the boundary condition applied for the free surface in the continuum is:

$$k\frac{\partial T}{\partial n}-\dot{q}_s+h(T-T_a)+\sigma\varepsilon\left(T^4-T_a^4\right)=0 \tag{6}$$

where n is the vector normal to the surface, $\dot{q}_s$ is the rate of heat input to the molten pool from the electric arc, h is the heat transfer coefficient, σ is the Stefan-Boltzmann constant, and ε is the emissivity.

4.2.1.1 Material models. Detailed information on thermo-physical properties of the material of component is essential to perform an accurate thermo-mechanical modelling. Since there is a thermal interaction between the power source and powder material in the process causing the melting of the feedstock requires information of temperature dependent inputs for the sensible as well as latent heat additions. The thermo-physical properties i.e., temperature dependent density, thermal conductivity, and specific heat contribute in the stability of the modelling practices considerably (Schoinochoritis *et al.*, 2014). However, other properties like Young's modulus, yield strength, and coefficient of thermal expansion can also be used in the simulation process, wherever required, to obtain accurate results (Jiang *et al.*, 2002; Van Belle *et al.*, 2012; Zaeh and Branner, 2010).

Among all thermo-physical properties, density is most important as it can influence other properties like thermal conductivity (Cervera and Lombera, 1999) and laser absorptivity of powder (Gibson *et al.*, 2009). For PBF AM processes, density can be affected by process time and temperature (Cervera and Lombera, 1999) and deposition rate (Childs *et al.*, 2000). The powder bed porosity has a strong impact on powder bed density. The particle size distribution, shape and size have an influence on the neck formation while solidification between the particles. Therefore, the density is mainly controlled by the bonding between the layers (Xiao and Zhang, 2007). Bauereiß *et al.* (2014) assumed that the relative density of powder material can vary between 40 and 60 per cent of the solid material. However, Nelson *et al.* (1993) and Childs *et al.* (1999) calculated the density variation in z direction using the following equation:

$$\frac{d\rho}{dt}=(\rho_{solid}-\rho)\cdot A\cdot e^{\left(\frac{-E}{RT}\right)} \tag{7}$$

where ρ_{soild} is the density of solid form of the powder material used, "A" is the sintering pre-exponential factor of the material, "E" is the activation energy, "R" is the universal gas constant, and "T" is the temperature. Dong *et al.* (2009) used a backward difference algorithm where $d\rho/d\,t = (\rho_{t+\Delta t}-\rho_t)/\Delta t$ has been substituted in the above equation. Therefore, the variation in density can be calculated as:

$$\rho_{t+\Delta t}=\frac{\rho_t+\Delta t\,.\,\rho_{solid}\,.\,A\,.\,e^{\left(\frac{-E}{RT}\right)}}{1+\Delta t\,.\,A\,.\,e^{\left(\frac{-E}{RT}\right)}} \tag{8}$$

The thermal conductivity of the powder particles on the substrate is very significant and complicated for accurate modelling of the process. Therefore, the thermal conductivity of the powder particle is described on the basis of powder solid relationship developed and used for the calculation of thermal conductivity of powder by Sih and Barlow (1994, 1995, 2004). The developed equation is given as (taken from Sih and Barlow, 2004);

$$\begin{aligned}\frac{k}{k_g}=&\left(1-\sqrt{1-\varphi}\right)\left(1+\frac{\varphi k_R}{k_g}\right)\\&+\sqrt{1-\varphi}\left\{(1-\varphi)\left[\frac{2}{1-\frac{Bk_g}{k_s}}\left(\frac{B}{\left(1-\frac{Bk_g}{k_s}\right)^2}\left(1-\frac{k_g}{k_s}\right)\ln\frac{k_s}{Bk_g}\right.\right.\right.\\&\left.\left.\left.-\frac{B+1}{2}-\frac{B-1}{1-\frac{Bk_g}{k_s}}\right)+\frac{K_R}{K_g}\right]+\phi\,\frac{k_{contact}}{k_g}\right\}\end{aligned} \tag{9}$$

In the above equation, k is the effective thermal conductivity of the powder material, k_g is the thermal conductivity of the continuous gas phase, k_s is the thermal conductivity of the skeletal solid, φ is the powder bed porosity, k_R is the thermal conductivity of the powder bed owing to radiation, ϕ is the flattened surface fraction in contact with another particle, B is the deformation parameter of the particle and it can be calculated by:

$$B\approx 1.25\left(\sqrt[\frac{10}{9}]{\frac{1-\varphi}{\varphi}}\right) \tag{10}$$

and:

$$k_R=\frac{4}{3}\sigma T^3 D_p \tag{11}$$

where D_p is the average diameter of the powder particle.

Apart from that, Yagi and Kunii (2004) derived a relation for effective thermal conductivity of the packed powder bed as per the following equation:

$$k_{eff}=\frac{\rho_r\,.\,k_s(T)}{1+\Phi\,.\,k_s(T)/k_g} \tag{12}$$

where, ρ_r is the relative density of the powder bed, $k_s\,(T)$ is the thermal conductivity of the solid material as a function of temperature, k_g is the thermal conductivity of surrounding gas and Φ is the empirical coefficient having value $0.02\,X\,10^{2(0.7-\rho_r)}$. Another model is given by Childs *et al.*

(Childs *et al.*, 1999) as a function of heat conductivity of solid material ($k_s(T)$) and porosity β:

$$k_{eff} = k_s(T).\left(1 - 0.2\beta - 1.73\beta^2\right) \quad (13)$$

In general, *specific heat* is non-linearly dependent on the change in temperature and phase transformation (Chen and Zhang, 2006). Since non-linear relationship requires large computational time therefore to reduce the complexity of the model, linear or interpolation function of temperature has been assumed as the specific heat of material at different temperature points (Dai and Shaw, 2002; Liu *et al.*, 2012; Li and Gu, 2014). Alternatively, the specific heat capacity of the powder bed can be found out considering powder bulk density by applying the law of Kopp-Neumann (Ren *et al.*, 2010).

4.2.1.2 Modelling assumptions. Simulation of the multi physics processes that occur in this process of melting and solidification in metal AM processes (shown in Figure 8) that affect the thermal cycle requires a lot of computational efforts. In such processes, many of the initial approaches calculating the thermal fields based on the various simplifications and assumptions to provide ease in the calculations. Some of the various important assumptions are complete heating then cooling (Nickel *et al.*, 2001), 2 D models (Vasinonta *et al.*, 2007; Matsumoto *et al.*, 2002; Foteinopoulos *et al.*, 2018), single layer approximation (Ghosh and Choi, 2005; Ocelik *et al.*, 2009; Matsumoto *et al.*, 2002), constant thermo-physical properties (Mukherjee *et al.*, 2017b; Denlinger and Michaleris, 2015; Mukherjee *et al.*, 2018; Das and Chung, 2001), neglecting convection and radiation (Foteinopoulos *et al.*, 2018; Hofmeister *et al.*, 1999; Das and Chung, 2001), neglecting loss of alloying elements (Mukherjee *et al.*, 2017b; Bai *et al.*, 2018; Mukherjee *et al.*, 2018), flat surface assumption for every layer (Mukherjee *et al.*, 2017b, 2018), Newtonian flow in molten pool (Bai *et al.*, 2018), and neglecting solid state phase transfer (Mukherjee *et al.*, 2018).

4.2.1.3 Moving heat source modelling. Heat source modelling is an important part of the thermo-mechanical models in PBF AM processes. Although some researchers directly used heat source as temperature load (Ma and Bin, 2007; Li *et al.*, 2016; Schilp *et al.*, 2014) but an important choice among the research community is Gaussian heat source models as a distributed heat source for the better accountability of physics involved. A diagram of Gaussian heat intensity distribution is shown in Figure 10 and the mathematical relation between heat flux

Figure 10 Gaussian distributed heat source

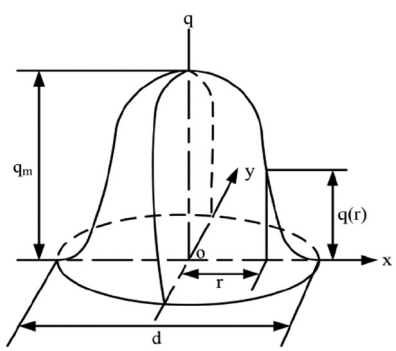

intensity q_{arc} of heat flux and the radial distance from the arc centre r_Q is given as (Ogino *et al.*, 2018):

$$q_{arc} = \frac{3Q_{arc}}{\pi r_Q^2} e^{\frac{-3r^2}{r_Q^2}} \quad (14)$$

where Q is the amount of heat transfer to the base, "r" is the centre radius of the arc.

Goldak *et al.* (1984) recommended a double ellipsoidal power density distribution considers the digging action of high-power density beams. On the experimental calculation of temperature gradient in front and back of the heat source, it has been discovered that the gradient is not equal for both sides. Therefore, two separate equations suggested for the front and rear sides of the molten pool.

$$q(x,y,z,t) = \frac{6\sqrt{3}f_f Q}{abc\pi\sqrt{\pi}} e^{\frac{-3x^2}{a^2}} e^{\frac{-3y^2}{b^2}} e^{\frac{-3[z+v(\tau-t)]^2}{c^2}} \quad (15)$$

$$q(x,y,z,t) = \frac{6\sqrt{3}f_r Q}{abc\pi\sqrt{\pi}} e^{\frac{-3x^2}{a^2}} e^{\frac{-3y^2}{b^2}} e^{\frac{-3[z+v(\tau-t)]^2}{c^2}} \quad (16)$$

In this model, the fraction of heat deposited f_f and f_r in front and rear quadrant can be considered as $f_f + f_r = 2$.

4.2.1.4 Meshing. Considering governing equations and few simplifications in the model solving, different computer based generalised FEM packages like ABAQUS (Mukherjee *et al.*, 2018; Tripathy *et al.*, 2017; Wu *et al.*, 2017; Shen and Chou, 2012), ANSYS (Dai and Shaw, 2001; Schilp *et al.*, 2014; Kamara *et al.*, 2011), and some specialised packages are like COMSOL (Masoomi *et al.*, 2017; La Batut *et al.*, 2017; Peyre *et al.*, 2008), CUBES (Pan computing LLC) (Denlinger *et al.*, 2014a; Denlinger and Michaleris, 2015), Deal.II (open source FEM library) (Riedlbauer *et al.*, 2014), Fluent (Dai and Gu, 2013), and SysWeld (Wang and Felicelli, 2007) are used by researchers across the world. However, the precision of the results in Finite Element Analysis (FEA) mainly depends on the type and configuration of the meshing system adopted for the analysis. Since computational cost and time are the major consideration in thermo-mechanical modelling, meshing strategy plays an important role to reduce the same with an effective measure. But still, adopting coarse meshes can cause the loss of physical contribution and error in the results obtained. Therefore, multi-resolution approaches, i.e. adaptive mesh refinement (AMR) and forms of embedded grids are contributing higher resolution in the area of active material transformation. AMR is basically the non-uniform mesh scheme that can fill the region of interest with denser meshes. According to mesh updation during processing, AMR is further divided into static AMR and dynamic AMR. As per the meshing scheme adopted, dynamic AMR can change the mesh density according to the value of the thermal gradient. As far as the uniform meshing [Figure 11(a)] is considered, they easy to implement and provide better and accurate results whereas to obtain better results fine meshing and a larger number of elements are required in this category which incurs high computational cost (Matsumoto *et al.*, 2002; Ma and Bin, 2007; Dai and Shaw, 2002; Patil and Yadava, 2007). While static AMR [Figure 11(b)] and dynamic AMR [Figure 11(c)]

Figure 11 Meshing schemes adopted to PBF AM

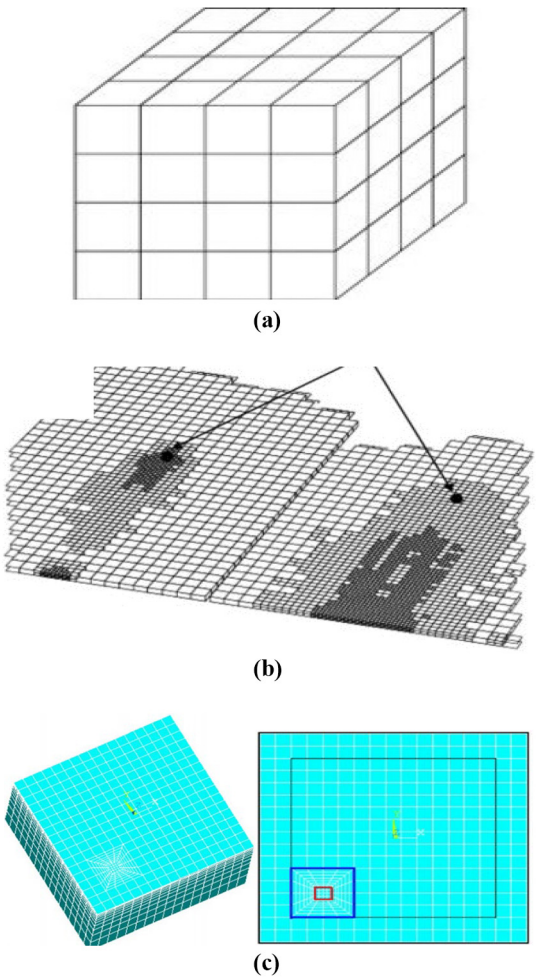

Source: Zeng *et al.* (2015)

incurs low computational cost and time because of lesser number of elements required for the analysis i.e. the denser meshing is only required for the consolidated area where heat source is interpolating as per the CAD model of the component (Hussein *et al.*, 2013; Antony *et al.*, 2014).

4.2.1.5 Element birth and death. The material in its powder or liquid form does not contribute to the overall stiffness of the model. To predict the accurate results of the model i.e. residual stress and distortion, the overall stiffness has to be considered into the model. To simulate the powder-liquid-solid transformation, there are two candidates to serve the purpose and yield accurate results, commonly known as Quiet Method and Inactive or the Dead Alive method (Lindgren and Hedblom, 2001; Michaleris, 2014). In the quiet method, elements present in the analysis is provided with their properties at the very start of analysis so that they cannot affect the surrounding structure and assigned with the real properties at the time the corresponding particle or elements are exposed to heat source, but in the inactive or dead alive method, a particle is not assigned with its properties until the particle is not actually exposed to the heat source (Lindgren and Hedblom, 2001). Element Birth and Death method is another name of Dead Alive method, mentioned in ANSYS finite element analysis software (Roberts *et al.*, 2009; Ren *et al.*, 2010). The elements are visually present in the model without adding to their overall stiffness as their actual stiffness is multiplied by a reduction factor (Denlinger *et al.*, 2014b). The actual stiffness has been retained by the deactivated elements after the solidification. A control mechanism decides the activation and deactivation of elements according to the temperature attained by the particular element. From a model building point of view, the application of element birth and death method i.e. controlling the state of the element and refining the mesh at each load step is a difficult and time-consuming task in the preparation of analysis.

4.2.1.6 Thermal boundary conditions. To quantify the exact amount of heat supply to the material on the substrate in the AM process, the heat addition and losses as well as the melting and solidification process should be modelled correctly by incorporating various boundary conditions applicable to the energy and mass transfer equations. Since metal AM processes are continuous layer and heat deposition process, heat losses may occur due to conduction through substrate and fixtures, losses due to radiation, free convection, and forced convection. However, if there is a large number of layers to be deposited, modelling losses through various heat transfer mechanisms is circumspect. In laser-based AM machines, since an inert gas is supplied as a medium for laser travel therefore forced convection is a dominating mode for the heat loss whereas in electron beam AM machines, a vacuum is required for electron beam travel, therefore only radiation is dominant mode of heat loss and should be carefully considered in the model building. It is a usual practice to club all heat transfer modes into a single overall heat transfer coefficient:

$$h_o = h_{fr} + h_{fo} + h_{rad} \tag{17}$$

and, overall heat transfer can be calculated as:

$$Q_O = h_o\,(T_s - T_\infty) \tag{18}$$

Where, h_o, h_{fr}, h_{fo}, h_{rad}, Q_O, T_s, T_∞ are overall heat transfer coefficient, free convective heat transfer coefficient, forced convective heat transfer coefficient, radiative heat transfer coefficient, convective heat transfer, surface temperature and ambient temperature respectively.

Convection can be considered the most significant mode of heat losses during the AM process except EBAM process, which necessarily takes place in a vacuum. It is well known that the mechanism of free convection is buoyant forces and the density differences in the stable molten pool which also causes the flow of molten metal from higher density towards lower density region. But the differences in density and buoyant forces are due to the thermal gradients which cause free convection in the AM process. Typical values of free convection can be considered between 5 and 15 W/m^2-°C (Gouge *et al.*, 2015; Heigel *et al.*, 2015). Lumped capacity analysis or the analytical modelling approach is usually used for the calculations of the free convection heat transfer coefficient.

Forced convection observed on the hot surface when gas flows over the surface with a temperature different from the

surface temperature. In the PBF process, forced convection takes place because of the inert gas environment provided in the chamber for the laser beam. Whereas, the DED process has dual gas flow i.e. shielding gas which provides shielding to the melt pool and gas used to drive the powder particle into the melt zone. The value of the forced convection heat transfer coefficient varies with the flow properties of the gases as well as with different systems. Since there is a possibility of turbulence due to high temperature difference between surfaces, can make the analytical modelling approach formidable. Yet there can be some approximation using the lumped capacitance for the average value of the heat transfer coefficient. An effective method of measuring near accurate values is to used hot wire or hot film anemometry experimentation in the particular system. Typical values of h_{fo} in the DED system can be considered in the range of 40-120 W/m^2 - °C (Gouge *et al.*, 2015; Heigel *et al.*, 2015). Whereas in LPBF systems, the values between 5 and 20 W/m^2 - °C, provides an accurate model result (Dunbar *et al.*, 2016b).

Radiation heat losses can be described by Stefan–Boltzmann law in PBF AM process and the mathematical equation is given as:

$$Q_r = \varepsilon\sigma\left(T_S^4 - T_\infty^4\right) \tag{19}$$

Where ε is surface emissivity and σ is Stefan–Boltzmann constant i.e. $\sigma = 5.67 \times 10^{-8}$ $W/m^2 - K^4$. In an absorbing and scattering medium, the angular radiation intensity is governed by the radiation transfer equation (RTE) (Baillis and Sacadura, 2000; Gusarov and Kruth, 2005; Gusarov *et al.*, 2009):

$$\Omega\nabla I = -(\sigma + \kappa)I + \frac{\sigma}{4\pi}\int_{4\pi} I(\Omega')\,P(\Omega' \rightarrow \Omega)d\,\Omega' \tag{20}$$

Where, σ and κ are the scattering and absorption coefficient respectively and $P(\Omega' \rightarrow \Omega)$ is the scattering phase function, which represents the probability of radiation moving in direction Ω' is scattered to direction Ω. The scattering phase function can be acquired by directional reflectivity of the powder material (Gusarov and Kruth, 2005) and for spherical metal particles, the reflection law with constant directional reflectivity can be suggested which gives isotropic scattering. Therefore, the phase can be normalised as:

$$\frac{1}{4\pi}\int_{4\pi} P(\Omega' \rightarrow \Omega)d\,\Omega' = 1 \tag{21}$$

In simplified cases, radiation is linearised and considered as potent heat transfer coefficient using the following simplifications;

$$Q_r = h_{rad}\left(T_s - T_\infty\right) \tag{22}$$

$$h_{rad} = \varepsilon\sigma\left(T_s + T_\infty\right)\left(T_s^2 + T_\infty^2\right) \tag{23}$$

Substrate and fixtures heat loss occurs due to the conduction mode of heat transfer. In LPBF systems, heat loss through build plate occurs due to conduction whereas in DED systems, conduction takes place through clamps and bolts which hold the substrate intact while fabrication is performed. In most cases conduction through substrate and fixture is neglected due to very small build volume or if the fixture contact is lesser comparatively. On the other hand, if the build volumes are comparatively larger and thin substrates, fixture losses should be included in the thermal model.

4.2.2 Mechanical modelling

The FE modelling of PBF AM processes consist of two different approaches i.e. non-linear transient thermal modelling and quasi-static elastoplastic mechanical analysis. A solution of thermal modelling by solving various conservation theorems is the temperature fields and velocity fields, which is needed as an input to mechanical modelling to predict the thermal stress and distortion developed in the part. The thermal-mechanical analysis can be performed in coupled or decoupled mode as shown in Figure 9. It can be seen in the figure that for coupled analysis, the thermal and mechanical analysis should be performed adjacently for each time step whereas, in uncoupled analysis, initially thermal analysis is performed and using its results in total, mechanical analysis has been performed (Gouge and Michaleris, 2018). Decoupled or weakly coupled are the favourite choice among the researchers due to the less computation cost (Roberts *et al.*, 2009; Dong *et al.*, 2009). The governing equation for stress equilibrium (Denlinger *et al.*, 2014a; Wang *et al.*, 2017; Dunbar *et al.*, 2016b) is given by:

$$\nabla \cdot \sigma = 0 \tag{24}$$

which further gives a constitutive equation in terms of stress, strain and material properties:

$$\sigma = C \cdot \epsilon^e \tag{25}$$

During continuous expansion and contraction due to variation in temperature, phase transformation (Li *et al.*, 2017), solid state phase transformation (Bartel *et al.*, 2019), and, inelastic effect due to plasticity and creep effect (Masubuchi, 1980) generates thermal strains in the fabricated part which in turn is the basic reason of residual stresses considering small deformation. The total strain observed in the fabricated part can be written as given in the equation:

$$\nabla\varepsilon_{ij}^{total} = \nabla\varepsilon_{ij}^{e} + \nabla\varepsilon_{ij}^{th} + \nabla\varepsilon_{ij}^{P} + \nabla\varepsilon_{ij}^{C} \tag{26}$$

$\nabla\varepsilon_{ij}^{e}$ is the elastic strain increment, $\nabla\varepsilon_{ij}^{th}$ is the thermal strains increment includes the effect of thermal gradient and phase transformation, $\nabla\varepsilon_{ij}^{P}$ is the plastic strain increment and $\nabla\varepsilon_{ij}^{C}$ is the strain occurred due to the creep. Kamara *et al.* (2011) recommended that the effect of creep can be neglected due to its short nature of time spent at high temperatures. Therefore, equation (xvii) can be modified neglecting the strain due to creep effect:

$$\nabla\varepsilon_{ij}^{total} = \nabla\varepsilon_{ij}^{e} + \nabla\varepsilon_{ij}^{th} + \nabla\varepsilon_{ij}^{P} \tag{27}$$

Gouge and Michaleris (2018) suggested that the thermal strains can be calculated by considering simple thermal strain and temperature relationship whereas plastic strains can be calculated by the Von-Mises yield criterion and Prandtl–Reuss flow rule:

$$\varepsilon_T = \varepsilon_T \mathbf{j} \tag{28}$$

$$\varepsilon_T = \alpha (T - T^{ref}) \tag{29}$$

$$j = [1\,1\,1\,0\,0\,0]^{\mathrm{T}} \tag{30}$$

In the above equations, α is the thermal expansion coefficient, T^{ref} is the reference temperature and ε_T is the thermal strain:

$$Y = \sigma_m - \sigma_y (\varepsilon_q, T) \leq 0 \tag{31}$$

$$\dot{\varepsilon}_P = \dot{\varepsilon}_q a \tag{32}$$

$$a = \left(\frac{\partial y}{\partial \sigma}\right)^T \tag{33}$$

Here, Y is the yield function, σ_m is the Mises' stress, σ_y is the yield stress, ε_q is the equivalent plastic strain and "a" is the flow vector.

4.2.2.1 Mechanical boundary conditions. The boundary conditions applicable to mechanical simulations are only the nodal constraints in the mechanical analysis. Importantly, all the nodes of substrate lower surface are rigidly constrained (Keller and Ploshikhin, 2014; Papadakis *et al.*, 2014), but few nodes are to be applied with spring constraints for the inclusion of elasticity to the clamps/supports (Denlinger *et al.*, 2014a). The final distortion can be obtained only after the component is fully cooled reaching the room temperature as well as clamps and supports are removed and to remove the base plate and removal of supports and clamps, there is a requirement of additional model which will simulate the removal of support and base plate from the build component (Papadakis *et al.*, 2014). This can be done by applying supplementary thermal loads or by disabling the elements at the lower base of the substrate.

4.3 Simulation results

4.3.1 Residual stress and distortion – prediction

Thermal stresses generated in the part when the volume of the body is not free to expand or contract due to temperature changes. To numerically find the value of residual stress and distortion, an elastoplastic or mechanical simulation is performed considering temperature profile obtained through thermal modelling as an input. In the process of melting and solidification, compressive stress is generated during the melting process converts into tensile form while solidification. Such variation in the nature of stress can be accredited to the comparatively high thermal expansion of the melt pool and its nearby area at high temperature. An effect of melt pool size has been investigated by Aggarangsi *et al.* (2003) with the increase of vertical free edge along with tensile stress in the vertical direction at the free edges and simulation result shows an effect of melt pool size on the stresses distribution on the free edges.

Dai and Shaw (2001) in their study investigated the effect of scanning patterns, fabrication sequence and scanning rates on the temperature and residual stress on the processing of multi-material components and given a basis of inter-relation of various parameters used in the study. They have found out while fabricating nickel and porcelain multi-structure component, scanning perpendicular to the interface produces more residual stress than scanning parallel to the interface while increasing the laser scanning rates causing an increase from 2 per cent to 62 per cent of maximum tensile stress and 8 per cent to 17 per cent of maximum compressive stress in the parallel scanning to the interface and it is also supported by Li *et al.* (2018c). A scalable predictive model has been developed by C. Li et al (Li *et al.*, 2018b) includes a microscale laser scan model, mesoscale layer hatch model, and macroscale part building model. The predicted residual stress is in good agreement with the experimental data in the suggested model i.e. a maximum distortion of 200 μm in the X and Y direction whereas 28 μm in the Z direction has been observed. Additionally, 400 MPa tensile residual stress predicted at the edge of the part. Further, Ali *et al.* (2018) investigates the effect of scanning strategy on SLM parts by varying size of the scan vector length, orientation of scan vectors, order of scanning and rotation of each subsequent layer. Seven scanning strategies had been adopted by the author to develop an optimum strategy with minimum possible residual stress and a 90° alternating strategy was chosen as an optimum as shown in Figure 12. The influence of scanning pattern as given by Ref. (Kruth *et al.*, 2004), i.e. the lengthwise scanning produces more residual stress with respect to the local island scanning consist of short scanning vectors whereas Parry *et al.* (2016) investigated the effect of scan strategies as well in the form unidirectional and alternating scanning in the longitudinal direction and they concluded the uniform distribution of plastic strain throughout the hatch region in unidirectional scanning [Figure 13(b)] while decreased plastic strains towards the end of scan when using alternating scan strategy [Figure 13(a)].

Warping and loss of edge tolerance are the effects of distortion in the part produced. The higher residual stresses are observed on the top surface and the interface between the substrate and part's lower surface (Van Belle *et al.*, 2012; Zaeh and Branner, 2010). Hodge *et al.* (2013) show that the high tensile stress has been generated at the top surface whereas, the bottom surface exhibits high compressive stresses that cause distortion and warping in the component. Moreover, Jiang *et al.* (2002) suggested that the part initially experiences compressive

Figure 12 Effect of scanning patterns on residual stress

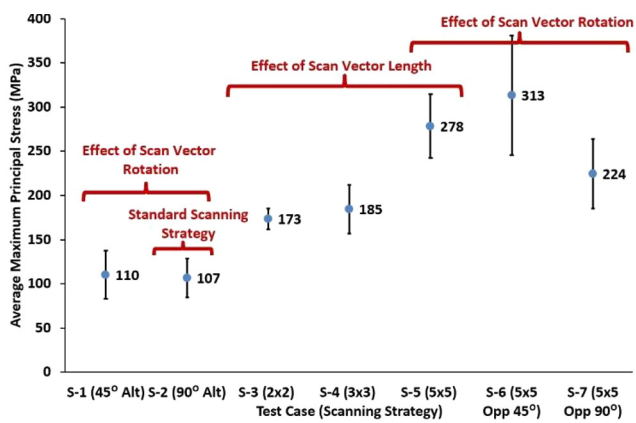

Source: Ali *et al.* (2018)

Figure 13 Total plastic strain fields

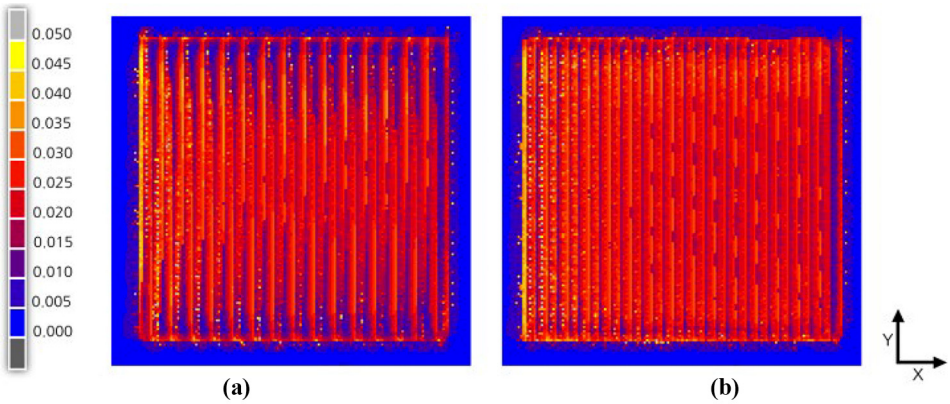

Source: Parry *et al.* (2016)

stresses gradually turns into tensile stress in the longitudinal direction after part cooling and distortion in the vertical direction is due to shrinkage of the powder while thermal gradients due to heat loading are the reason for horizontal warping of the part.

For the effect of process parameters of energy source and other process components, Corbin *et al.* (2016) assess the influence of substrate thickness, layer thickness, and initial base temperature on residual stress while keeping energy source parameters constant. In-situ measurement of thermal distortion has been carried out and they found that the preheating of the substrate decreases the total distortion by 22.1 per cent for thin substrate (2.54 mm) and increase of total distortion by 111.9 per cent for thick substrate (12.7 mm). Substrate and powder preheating have been given a great attention i.e. it leads to larger longitudinal compressive stress divisions at the lower side of the part (Papadakis *et al.*, 2012) whereas it also leads to higher tensile stress in the component (Krol *et al.*, 2013). A summarised review of important factors responsible for residual stress and distortion in the PBF AM process has been given in Table V.

4.3.2 Experimental validation

Real life experiments are required to validate the predicted results obtained through analytical or numerical models for PBF AM processes since some assumptions and simplifications are incorporated into the model. Therefore, some in-situ or post process measurement techniques explained in the next section, adopted for the measurement of temperature fields and melt pool geometry. In-situ measurement of residual stress and distortion is a difficult task. Hence, residual stress has been measured in the post processing of the component and the

Table V Important factors causing residual stress in AM builds

Important factors	Effects due to variations	Process (reference)
Temperature Distribution	High temperature gradients causing higher cooling rates lead to higher residual stress and distortion in the PBF AM builds	SLS (Ma and Bin, 2007), SLM (Wu *et al.*, 2017; Hussein *et al.*, 2013)
Substrate Preheating	The temperature gradient is reduced by the substrate preheating and thus cracking and layer delamination is prevented due to residual stress	Laser Densification (Dai *et al.*, 2004), LMD (Zhang *et al.*, 2014), SLM (Zaeh and Branner, 2010), SLM (Papadakis *et al.*, 2012), Krol *et al.*, 2013)
Substrate Thickness	The thicker substrate provides more stiffness to the builds and leads to lower and more uniform residual stress	LENS (Corbin *et al.*, 2016), EBM (Shen and Chou, 2012; Yagi and Kunii, 2004)
Scanning Speed/ Laser Exposure Time	High exposure of power source or low scanning speed causes more heat accumulation and higher cooling rates in AM builds	SLM (Hussein *et al.*, 2013), Laser Densification (Dai and Shaw, 2001)
Layer Thickness	Thin powder layers causing more thermal stresses and distortion in the builds	SLM (Mercelis and Kruth, 2006; Sufiiarov *et al.*, 2017), SDM (Nickel *et al.*, 1999)
Scanning Patterns	Scanning patterns have considerable influence on residual stress i.e., short scan paths like fractal or spiral or small island-based scanning causing a reduction in thermal stress	SLM (Ali *et al.*, 2018; Kruth *et al.*, 2004; Parry *et al.*, 2016; Li *et al.*, 2018c; Cheng *et al.*, 2016), Laser Densification (Dai and Shaw, 2001)
Power Input	Higher energy density causes an increase in change of strain in turn causing more residual stress	DED (Wang *et al.*, 2016), SLM (Jia and Gu, 2014)
Length of Scan	Longitudinal direction experiences more residual stress and distortion compared to transverse directions	SLM (Hussein *et al.*, 2013; Zaeh and Branner, 2010; Kruth *et al.*, 2004), Laser Densification (Dai and Shaw, 2001)

most famous non-destructive measurement technique is Neutron Diffraction (Wang *et al.*, 2017). To quantify the temperature profile during layer deposition, conventional temperature measurement techniques such as thermographic cameras and thermocouple (Usamentiaga *et al.*, 2014) are required. Most of the experiments performed for validation are for single tracks or for simple geometries i.e. thin wall structure, T-shape structure, circular thin wall etc. These structures do not consist of geometrical complexity of the slicing layer which can be a case of complicated industrial parts. Therefore, it is suggested to consider complex geometries for validation of developed models such as acute angle, overhung parts and hollow structures.

4.4 Residual stress and distortion – minimization and mitigation techniques

Residual stresses develop in almost all metal AM processes. The reason behind the generation of residual stresses in the components is the continuous contraction and expansion related to the deposition of sequential layers. This residual stress causes various kinds of defects, i.e. distortion, cracking and delamination. There are various metrological procedures to quantify the values of residual stress and distortion. Among these processes some of the non-destructive techniques i.e. X-ray diffraction (XRD) (Klingbeil *et al.*, 1997; Yadroitsev and Yadroitsev, 2015; Liu *et al.*, 2016; Fergani *et al.*, 2016) is of most use. Furthermore, strain gauges (Klingbeil *et al.*, 1997), M-DVRT displacement sensor (Dunbar *et al.*, 2016a), neutron diffraction (Wang *et al.*, 2017; Ghasri-Khouzani *et al.*, 2017; Szost *et al.*, 2016; Li *et al.*, 2018a) and distortion measurement through CMM (Ghasri-Khouzani *et al.*, 2017), electronic speckle pattern interferometry (Casavola *et al.*, 2017). Lu (1996) described almost every type of measurement procedure of residual stresses in the welding process which can be used in the case of AM processes. Residual stress itself causes various other defects in the AM builds. Therefore, it is recommended to mitigate or minimise its effects by controlling the factors which are responsible for its generation.

Chin *et al.* (1995) first reported the control of residual thermal stress in shaped metal deposition process by investigating the effect of substrate heating prior to newly applied droplets and the bending constraints on the build-up. Nickel *et al.* (1999) developed an analytical and FEM based model to investigate the effect of the number of layers, layer thickness and deposition pattern on the deflection of part produced. They have found that the elastic analytical model produces a deflection of 0.82 mm in Invar 23 and 6.21 mm in 1117 steel parts respectively as well as using the bending constraints in 1117 steel, deflection had been reduced to 0.16 mm. Apart from this, they have investigated the beam raster pattern to conclude that the short raster pattern produces a deflection of 0.44 mm in 1117 steel with respect to long raster produces a deflection of 1.00 mm at the same settings. In addition to that, results from Christmas tree step analysis provides an insight into the local deformation process that happens near the edges of many layered manufacturing process. Continuous efforts have been made till date to minimise the effect of residual stress in the AM builds so that the defects caused due to this can be controlled.

Vasinonta *et al.* (2000) have given two mechanisms to reduce the effect of residual stress viz., decreasing the strain mismatch (controlling the strain parameter developed by Mukherjee *et al.* (2017a) during cooling as the temperature gradient is also decreasing and reduction of yield stress. Localised preheating is the most accepted residual stress reduction method across the researchers' community which includes preheating around the melt-pool and substrate (Aggarangsi and Beuth, 2006; Yuan and Bourell, 2012; Ali *et al.*, 2017). Denlinger and Michaleris (2015) suggested that adding sacrificial material to the large components fabricated through electron beam AM consisting of several thousand layers considered to most effective as it reduced the longitudinal bending distortion by 91 per cent. Careful consideration and control of process parameters have also been considered by Jiang *et al.* (2002), Vatsola *et al.* (2016) to control the development of residual stress and distortion in the Ti6Al4V build through EBM.

The above findings indicate that the residual stresses in AM builds are mainly mitigated through substrate preheating, powder bed preheating, efficient scanning strategies, modifying various processes parameters, deposition strategies, reduction in yield stress and Fourier number etc. These can be an effective approach to deal with built or as built residual stress which further reduces the distortion in the part produced.

5. Modelling challenges – a future direction

Although several prominent methods are available to predict and characterise residual stress and distortion in PBF AM components. But, as Collins *et al.* (2016) in 2016 mentioned that the residual stress, either compressive or tensile, is capable of generating distortions and micro-cracks in the parts. Hence, a lot of research is being conducted on the defect modelling of metal AM parts these days, especially, distortion and residual stress has not been dealt in depth with respect to the properties of metal powder i.e. effect of the powder particle behaviour like powder packing density and particle shape on liquid flow, residual stress and distortion (Matthews *et al.*, 2016).

As control of residual stress is concerned, Stavropoulos and Foteinopoulos (2018) stated that since all metal AM processes uses heat as the mode of energy to bind layers together therefore, the key performance indicators (KPIs) related to heat addition and losses should be taken care of precisely to control the defects, mechanical properties, microstructure, and topology. Those KPIs should be improved to control the quality of components manufactured through the AM process. Various simplifications/assumptions adopted for thermo-mechanical models, has been failed to address the underlying physics and results in a deviation from the experimental observation. National AM Innovation Institute in its roadmap (America Makes, and ANSI – AMSC, 2017) provided gaps and recommendations for AM simulation benchmark model which suggests the development of canonical models that reproduce difficult to build features are needed for verification and validation along with the recommendations for precursor powder materials.

Modelling of Metal AM processes is a very challenging field. The modelling practices in metal AM have been split in to multi-scale i.e. macro-, micro- and meso-scales due to

variations in spatial and temporal scales that require the subdivisions. FEA can be a powerful tool to deal with these challenges to predict the mechanical performance by adjusting the respective process parameters. However, adopting FEA at an industrial domain is still challenging due to large computational time. Therefore, smart approaches should be incorporated to reduce model complexity without sacrificing the involved multi-physics. Some of the approaches have been discussed in this article. But, attention to the loss of considerable accuracy while adopting an alternate approach or implementation of the already developed model to the moderate to complex geometries are still not dealt in depth. Commercial FEA packages dedicated to AM modelling and simulation yields very limited capabilities to properly address the process complexity. The reason behind this is the requirement of highly qualified personal capable of performing complex "element birth and death" and "moving heat source" modelling, who can implement these into existing FEA packages.

Other challenges include heat accumulation during successive layer deposition causing an effect of the residual heat on the depositing layer due to the previously deposited layer, changes the convection state of the melt pool and current research trends in thermo-mechanical modelling shows that the study of thermal behaviour is restricted to single track handling. Therefore, in future, the effect of the residual heat of the deposited layer can be considered in the numerical models.

A few more future research directions, which was not found in the literature precisely or paid less attention, as suggested by authors are summarised below:

- an investigation of the effect of powder properties, i.e. powder packing density and particle shape on residual stress and distortion;
- measurement methods for micro/macro residual stress in PBF AM processes;
- development of in situ distortion mitigation techniques in PBF AM processes;
- consideration of solid-state phase transformation strains in thermo-mechanical models; and
- performance and characterisation of the part produced through the PBF AM process in fatigue, creep and corrosion environment against residual stresses.

6. Conclusion

Freedom of design, flexibility in customisation and complex geometries with almost negligible waste are the main attributes of metal AM technology. In this article, the existing AM processes as per ASTM/ISO 52900 and multi-physics continuum modelling approach for PBF AM processes have been presented. Furthermore, an exhaustive review on mesoscale modelling approach in the form of material supply modelling along with part-scale macro modelling incorporating heat and material supply, melting and solidification process to quantify residual stress and distortion produced in the part discussed in the article. On the basis of reviewed articles, the following points can be concluded:

- Maximum studies focussed on the laser-based PBF AM process while very few studies have been reported on EBAM.
- New materials and alloys need to be investigated as most studies have been performed on steel specimens.
- Studies on *in situ* characterisation of defects including residual stress are scant.
- Already published experimental results had been used for the experimental validation in most cases by researchers. Thus, new experiments have to be performed for a better understanding of the process.
- The development of computationally efficient models for long scale AM builds is required as there are very few cases reported. The application of dynamic AMC method in the PBF AM process is also very limited.

The FEM has been proved an asset in the simulation of metal AM process. The process can be adjusted and optimised to produce a fully functional component for the very first time by understanding the involved physical phenomena in the process and predicting the effect of process parameters on the mechanical properties of the final component. However, there are a lot of issues needs to be addressed i.e. long computational time does not allow the integration of FEA for online optimisation of the process. Finally, the total shift of manufacturing to a web-based and cloud-based manufacturing kick-starting the integrat ion of the FEA tool with other process optimisation tools so that the need for the current global manufacturing networks can be served.

References

3dexperience (2019), available at: https://make.3dexperience.3ds.com/processes/photopolymerization (accessed 18 June 2019).

3D Systems (2018), "3D systems SLA production series brochure", available at: www.3dsystems.com/sites/www.3dsystems.com/files/sla-series-0514-usen-web.pdf (accessed 27 March 2018).

Abe, F., Osakada, K., Shiomi, M., Uematsu, K. and Matsumoto, M. (2011), "The manufacturing of hard tools from metallic powders by selective laser melting", *Journal of Materials Processing Technology*, Vol. 111 Nos 1/3, pp. 210-213.

Additive3d (2020), The Rapid Prototyping Patent Museum: Basic Technology Patents. available at: www.additive3d.com/museum/mus_c.htm

Aggarangsi, P. and Beuth, J.L. (2006), "Localised preheating approaches for reducing residual stress in additive manufacturing", *Proceedings of the 16th Annual International Solid Freeform Fabrication Symposium – An Additive Manufacturing Conference, Solid Freeform Fabrication* pp. 709-720, available at: https://sffsymposium.engr.utexas.edu/Manuscripts/2006/2006-61-Aggarangsi.pdf

Aggarangsi, P., Beuth, J.L. and Griffith, M. (2003), "Melt Pool size and stress control for laser-based deposition near a free edge", *Proceedings of the 14th Annual International Solid Freeform Fabrication Symposium – An Additive Manufacturing Conference, Solid Freeform Fabrication* pp. 196-207, available at: http://sffsymposium.engr.utexas.edu/Manuscripts/2003/2003-18-Aggarangsi.pdf

Ali, H., Ghadbeigi, H. and Mumtaz, K. (2018), "Effect of scanning strategies on residual stress and mechanical

properties of selective laser melted Ti6Al4V", *Materials Science and Engineering: A*, Vol. 712, pp. 175-187.

Ali, H., Ma, L., Ghadbeigi, H. and Mumtaz, K. (2017), "In-situ residual stress reduction, martensitic decomposition and mechanical properties enhancement through high temperature powder bed pre-heating of selective laser melted Ti6Al4V", *Materials Science and Engineering: A*, Vol. 695, pp. 211-220.

AM Special Interest Group (2012), "Shaping our national competency in additive manufacturing", in T.S. Board (Ed.), UK Government.

America Makes, and ANSI – AMSC (2017), "Standardization roadmap for additive manufacturing – version 1.0", National Additive Manufacturing Innovation Institute, available at: https://share.ansi.org/Shared%20Documents/Standards%20Activities/AMSC/AMSC_Roadmap_February_2017.pdf

Anderson, D.M., McFadden, G.B. and Wheeler, A.A. (2000), "A phase-field model of solidification with convection", *Physica D: Nonlinear Phenomena*, Vol. 135 Nos 1/2, pp. 175-194.

Anderson, M.P., Srolovitz, D.J., Grest, G.S. and Sahni, P.S. (1984), "Computer simulation of grain growth – I. Kinetics", *Acta Metallurgica*, Vol. 32 No. 5, pp. 783-791.

Andersson, B.A.B. (1978), "Thermal stresses in a submerged arc welded joint considering phase transformation", *Journal of Engineering Materials and Technology*, Vol. 100 No. 4, pp. 356-362.

Antony, K., Arivazhagan, N. and Senthilkumaran, K. (2014), "Numerical and experimental investigations on laser melting of stainless steel 316L metal powders", *Journal of Manufacturing Processes*, Vol. 16 No. 3, pp. 345-355.

Argyris, J.H., Szimmat, J. and William, K.J. (1982), "Computational aspect of welding stress analysis", *Computer Methods in Applied Mechanics and Engineering*, Vol. 33 Nos 1/3, pp. 635-665.

ASTM Standard (2012), "Standard terminology for additive manufacturing technologies", *ASTM Standard F2792-12a*, ASTM International, West Conshohocken, PA.

Attar, E. and Körner, C. (2011), "Lattice boltzmann model for thermal free surface flows with liquid solid phase transition", *International Journal of Heat and Fluid Flow*, Vol. 32 No. 1, pp. 156-163.

Bai, X., Colegrove, P., Ding, J., Zhou, X., Diao, C., Bridgeman, P., Hönnige, J.R., Zhang, H. and Williams, S. (2018), "Numerical analysis of heat transfer and fluid flow in multilayer deposition of PAW-based wire and arc additive manufacturing", *International Journal of Heat and Mass Transfer*, Vol. 124, pp. 504-516.

Baillis, D. and Sacadura, J.F. (2000), "Thermal radiation properties of dispersed media: theoretical prediction and experimental characterization", *Journal of Quantitative Spectroscopy and Radiative Transfer*, Vol. 67 No. 5, pp. 327-363.

Baran, A. and Polanski, M. (2018), "Microstructure and properties of LENS (laser engineered net shaping) manufactured NI-Ti shape memory alloy", *Journal of Alloys and Compounds*, Vol. 750, pp. 863-870.

Bartel, T., Guschke, I. and Menzel, A. (2019), "Towards the simulation of selective laser melting processes via phase transformation models", *Computers & Mathematics with Applications*, Vol. 78 No. 7, pp. 2267-2281.

Bauereiß, A., Scharowsky, T. and Körner, C. (2014), "Defect generation and propagation mechanism during additive manufacturing by selective beam melting", *Journal of Materials Processing Technology*, Vol. 214 No. 11, pp. 2522-2528.

Baykasoglu, C., Akyildiz, O., Candemir, D., Yang, Q., C. and To, A. (2018), "Predicting microstructure evolution during directed energy deposition additive manufacturing of Ti-6Al-4V", *Journal of Manufacturing Science and Engineering*, Vol. 140 No. 5, pp. 051003-1–051003-11.

Beaman, J.J., Barlow, J.W., Bourell, D.L., Crawford, R.H., Marcus, H.L. and McAlea, K.P. (1996), *Solid Freeform Fabrication: A New Direction in Manufacturing*, Springer, New York, NY. https://doi.org/10.1007/978-1-4615-6327-3

Bikas, H., Stavropoulos, P. and Chryssolouris, G. (2016), "Additive manufacturing methods and modelling approaches: a critical review", *The International Journal of Advanced Manufacturing Technology*, Vol. 83 Nos 1/4, pp. 389-405.

Boley, C.D. and Rubenchik, A.M. (2013), "Modelling of laser interaction with composite materials", *Applied Optics*, Vol. 52 No. 14, pp. 3329-3337.

Boley, C.D., Khairallah, S.A. and Rubenchik, A.M. (2015), "Calculation of laser absorption by metal powders in additive manufacturing", *Applied Optics*, Vol. 54 No. 9, pp. 2477-2482.

Bose, S., Vahabzadeh, S. and Bandyopadhyay, A. (2013), "Bone tissue engineering using 3D printing", *Materials Today*, Vol. 16 No. 12, pp. 496-504.

Bourell, D.L., Beaman, J., Jr, Klosterman, D., Gibson, I. and Bandyopadhyay, A. (2001), "Rapid prototyping", *ASM Handbook Composites*, Vol. 21, pp. 383-387. https://doi.org/10.1361/asmhba0003397

Brice, C.A., Rosenberger, B.T., Sankaran, S.N., Taminger, K.M., Woods, B. and Nasserrafi, R. (2009), "Chemistry control in electron beam deposited titanium alloys", *Materials Science Forum*, Vol. 618 No. 9, pp. 155-158.

Brown, S.B. and Song, H. (1992), "Implication of three-dimensional numerical simulations of welding of large structures", *Welding Journal*, Vol. 71 No. 2, pp. 55s–62s, available at: https://app.aws.org/wj/supplement/WJ_1992_02_s55.pdf

Buchbinder, D., Schleifenbaum, H., Heidrich, S., Meiners, W. and Bültmann, J. (2011), "High power selective laser melting (HP SLM) of aluminium parts", *Physics Procedia*, Vol. 12, pp. 271-278.

Cao, X., Wallace, W., Poon, C. and Immarigeon, J.P. (2007), "Research and progress in laser welding of wrought aluminium alloys. I. Laser welding process", *Materials and Manufacturing Processes*, Vol. 18 No. 1, pp. 1-22.

Carter, L.N., Attallah, M.M. and Reed, R.C. (2012), "Laser powder bed fabrication of nickel-base superalloys: influence of parameters; characterisation, quantification and mitigation of cracking", *Super-alloys 2012 - 12th International Symposium on Super-alloys*, pp. 577-586, available at: https://doi.org/10.1002/9781118516430.ch64

Casavola, C., Cazzato, A., Moramarco, V. and Pappalettera, G. (2017), "Residual stress measurement in fused deposition modelling parts", *Polymer Testing*, Vol. 58, pp. 249-255.

Cervera, G.B.M. and Lombera, G. (1999), "Numerical prediction of temperature and density distributions in selective laser sintering processes", *Rapid Prototyping Journal*, Vol. 5 No. 1, pp. 21-26.

Cesarano, J. (1999), "A review of robocasting technology", *Material Research Society Symposium Proceedings*, Vol. 542, pp. 133-139. , available at: https://doi.org/10.1557/PROC-542-133

Cesarano, J., Baer, T.A. and Calvert, P. (1997), "Recent developments in freeform fabrication of dense ceramics from slurry deposition", *8th International solid freeform fabrication symposium*, pp. 25-32, available at: https://sffsymposium.engr.utexas.edu/Manuscripts/1997/1997-04-Cesarano.pdf

Chen, T. and Zhang, Y. (2004), "Numerical simulations of two-dimensional melting and re-solidification of a two-component metal powder layer in selective laser sintering process", *Numerical Heat Transfer, Part A: Application*, Vol. 46 No. 7, pp. 633-649.

Chen, T. and Zhang, Y. (2006), "Three-dimensional modelling of laser sintering of two-component metal powder layer on top of sintered layer", *Journal of Manufacturing Science and Engineering*, Vol. 129 No. 3, pp. 575-582.

Chen, C., Shen, Y. and Tsai, H.L. (2016), "A foil based additive manufacturing technology for metal parts", *Journal of Manufacturing Science and Engineering*, Vol. 139 No. 2, pp. 1188-1193.

Chen, Z., Ye, H. and Xu, H. (2018), "Distortion control in a wire-fed electron-beam thin-walled Ti-6Al-4V freeform", *Journal of Materials Processing Technology*, Vol. 258, pp. 286-295.

Cheng, B., Shrestha, S. and Chou, K. (2016), "Stress and deformation evaluations of scanning strategy effect in selective laser melting", *Additive Manufacturing*, Vol. 12, pp. 240-251.

Childs, T.H.C., Berzins, M., Ryder, G.R. and Tontowi, A.E. (1999), "Selective laser sintering of an amorphous polymer – simulations and experiments", *Journal of Engineering Manufacture*, Vol. 213 No. 4, pp. 333-349.

Childs, T.H.C., Hauser, C., Taylor, C.M. and Tontowi, A. E. (2000), "Simulation and experimental verification of crystalline polymer and direct metal selective laser sintering", *Proceedings of the 11th Annual International Solid Freeform Fabrication* Symposium – An Additive Manufacturing Conference, Solid Freeform Fabrication pp. 200-208, available at: https://sffsymposium.engr.utexas.edu/Manuscripts/2000/2000-13-Childs.pdf

Chin, R.K., Beuth, J.L. and Amon, C.H. (1995), "Control of residual thermal stresses in shape metal deposition", *6th Annual International Solid Freeform Fabrication Symposium* pp. 221-228, available at: http://sffsymposium.engr.utexas.edu/Manuscripts/1995/1995-27-Chin.pdf

Chin, R.K., Beuth, J.L. and Amon, C.H. (1996a), "Thermo-mechanical modelling of molten metal droplet solidification applied to layered manufacturing", *Mechanics of Materials*, Vol. 24 No. 4, pp. 257-271.

Chin, R.K., Beuth, J.L. and Amon, C.H. (1996b), "Thermo-mechanical modelling of successive material deposition in layered manufacturing", *7th Annual International Solid Freeform Fabrication Symposium*, University of TX pp. 507-514, available at: https://sffsymposium.engr.utexas.edu/Manuscripts/1996/1996-59-Chin.pdf

Chryssolouris, E.L.K.E. (2015), *Manufacturing Systems: theory and Practice*, 2nd edition. Springer, New York, NY. https://doi.org/10.1007/0-387-28431-1

Chua, C.K., Leong, K.F. and Lim, C.S. (2010), *Rapid Prototyping: Principles and Applications*, 3rd ed., World Scientific Publishing Company, Singapore, pp. 165-171. https://doi.org/10.1142/9789812778994_0003

Collins, P.C., Brice, D.A., Samimi, P., Ghamarian, I. and Fraser, S.L. (2016), "Microstructural control of additively manufactured metallic materials", *Annual Review of Materials Research*, Vol. 46 No. 1, pp. 63-91.

Corbel, S., Allanic, A.L., Schaeffer, P. and Andre, J.C. (1994), "Computer aided manufacture of three-dimensional objects by laser shaped resolved polymerization", *Journal of Intelligent & Robotic Systems*, Vol. 9 No. 3, pp. 301-312.

Corbin, D.J., Nassar, A.R., Reutzel, E.W., Kistler, N.A., Beese, A.M. and Michaleris, P. (2016), "Impact of directed energy deposition parameters on mechanical distortion of laser deposited Ti-6Al-4V", *27th Annual International Solid Freeform Fabrication Symposium – An Additive Manufacturing Conference, Solid Freeform Fabrication* pp. 670-679, available at: http://sffsymposium.engr.utexas.edu/sites/default/files/2016/051-Corbin.pdf

Cundall, P.A. and Strack, O.D.L. (1979), "A discrete numerical model for granular assemblies", *Géotechnique*, Vol. 29 No. 1, pp. 47-65.

Dahotre, N.B. and Harimkar, S. (2008), *Laser Fabrication and Machining of Materials*, Springer, New York, NY, available at: https://doi.org/10.1007/978-0-387-72344-0

Dai, D. and Gu, D. (2013), "Thermal behaviour and densification mechanism during selective laser melting of copper matrix composites: simulation and experiments", *Materials & Design*, Vol. 55, pp. 482-491.

Dai, K. and Shaw, L. (2001), "Thermal and stress modelling of laser fabrication of multiple material component", *12th Annual International Solid Freeform Fabrication Symposium*, University of TX pp. 330-337, available at: https://sffsymposium.engr.utexas.edu/Manuscripts/2001/2001-37-DaiShaw.pdf

Dai, K. and Shaw, L. (2002), "Distortion minimization of laser-processed components through control of laser scanning patterns", *Rapid Prototyping Journal*, Vol. 8 No. 5, pp. 270-276.

Dai, K., Li, X.X. and Sham, L.L. (2004), "Comparison between thermal modelling and experiments: effects of substrate *p* reheating", *Rapid Prototyping Journal*, Vol. 10 No. 1, pp. 24-34.

Darvish, K., Chen, Z.W. and Pasang, T. (2016), "Reducing lack of fusion during selective laser melting of CoCrMo alloy: effect of laser power on geometrical features of tracks", *Materials & Design*, Vol. 112, pp. 357-366.

Das, S. and Chung, H. (2001), "A model of laser-powder interaction in direct selective laser sintering of metals", *12th Annual International Solid Freeform Fabrication*

Symposium, available at: https://sffsymposium.engr.utexas.edu/Manuscripts/2001/2001-40-Das.pdf

Deng, X.L. and Davè, R.N. (2013), "Dynamic simulation of particle packing influenced by size, aspect ratio and surface energy", *Granular Matter*, Vol. 15 No. 4, pp. 401-415.

Denlinger, E.R. and Michaleris, P. (2015), "Mitigation of distortion in large additive manufacturing parts", *Journal of Engineering Manufacture*, Vol. 231 No. 6, pp. 983-993.

Denlinger, E.R., Heigel, J.C. and Michaleris, P. (2014b), "Residual stress and distortion modelling of electron beam direct manufacturing Ti-6Al-4V", *Journal of Engineering Manufacture*, Vol. 229 No. 10, pp. 1803-1813.

Denlinger, E.R., Irwin, J. and Michaleris, P. (2014a), "Thermomechanical modelling of additive manufacturing large parts", *Journal of Manufacturing Science and Engineering*, Vol. 136 No. 6, 061007-1-061007-8.

Dong, L., Makradi, A., Ahzi, S. and Remond, Y. (2009), "Three-dimensional transient finite element analysis of the selective laser sintering process", *Journal of Materials Processing Technology*, Vol. 209 No. 2, pp. 700-706.

Dunbar, A.J., Denlinger, E.R., Gouge, M.F. and Michaleris, P. (2016b), "Experimental validation of finite element modelling for laser powder bed fusion deformation", *Additive Manufacturing*, Vol. 12 No. A, pp. 108-120.

Dunbar, A.J., Denlinger, E.R., Heigel, J., Michaleris, P., Guerrier, P., Martukanitz, R. and Simpson, T.W. (2016a), "Development of experimental method for in situ distortion and temperature measurements during the laser powder bed fusion additive manufacturing process", *Additive Manufacturing*, Vol. 12, pp. 25-30.

Eymard, R., Gallouët, T. and Herbin, R. (2000), "Finite volume methods", *Handbook of Numerical Analysis*, Vol. 7, pp. 713-1018, Available at: https://doi.org/10.1016/S1570-8659(00)07005-8

Fan, Z. and Liou, F. (2012), "Numerical modelling of the additive manufacturing (AM) processes of titanium alloy", in Nurul Amin, A K M. (Ed.), *Titanium Alloys - Towards Achieving Enhanced Properties for Diversified Applications*, Intechopen, London pp. 4-28, Available at: https://doi.org/10.5772/34848

Fergani, O., Berto, F., Welo, T. and Liang, S.Y. (2016), "Analytical modelling of residual stress in additive manufacturing", *Fatigue & Fracture of Engineering Materials & Structures*, Vol. 40 No. 6, pp. 971-978.

Fina, F., Goyanes, A., Madla, C.M., Awad, A., Trenfield, S.J., Kuek, J.M., Patel, P., Gaisford, S. and Basit, A.W. (2018), "3D printing of drug loaded gyroid lattice using selective laser sintering", *International Journal of Pharmaceutics*, Vol. 547 No. 1-2, pp. 44-52.

Foteinopoulos, P., Papacharalampopoulos, A. and Stavropoulos, P. (2018), "On thermal modelling of additive manufacturing processes", *CIRP Journal of Manufacturing Science and Technology*, Vol. 20, pp. 66-83.

Francois, M.M., Amy, S., King, W.E. and Henson, N.J. (2017), "Modelling of additive manufacturing processes for metals: challenges and opportunities", *Current Opinion in Solid State and Materials Science*, Vol. 21 No. 4, pp. 198-206.

Frazier, W.E. (2014), "Metal additive manufacturing: a review", *Journal of Materials Engineering and Performance*, Vol. 23 No. 6, pp. 1917-1928.

Gandolfi, M.G., Zamparini, F., Esposti, M.D., Chiellini, F., Aparicio, C., Fava, F., Fabbri, P., Taddei, P. and Prati, C. (2018), "Polylactic acid based porous scaffolds doped with calcium silicate and dicalcium phosphate dehydrate designed for biomedical application", *Materials Science and Engineering: C*, Vol. 82, pp. 163-181.

Ghasri-Khouzani, M., Peng, H., Rogge, R., Attardo, R., Ostiguy, P., Neidig, J., Billo, R., Hoelzle, D. and Shankar, M.R. (2017), "Experimental measurement of residual stress and distortion in additively manufactured components with various dimensions", *Materials Science and Engineering: A*, Vol. 707, pp. 689-700.

Ghosh, S. and Choi, J. (2005), "Three-dimensional transient finite element analysis for residual stresses in the laser aided direct metal/material deposition process", *Journal of Laser Applications*, Vol. 17 No. 3, pp. 144-158.

Gibson, I., Rosen, D.W. and Stucker, B. (2009), *Additive Manufacturing Technologies: Rapid Prototyping to Direct Digital Manufacturing*, Springer, New York, NY, Available at: https://doi.org/10.1007/978-1-4419-1120-9

Goldak, J., Chakravarti, A. and Bibby, M. (1984), "A new finite element model for welding heat source", *Metallurgical Transactions B*, Vol. 15 No. 2, pp. 299-305.

Gouge, M. and Michaleris, P. (2018), *Thermo-Mechanical Modelling of Additive Manufacturing*, Elsevier Inc, Butterworth-Heinemann, Oxford available at: https://doi.org/10.1016/B978-0-12-811820-7.00003-3

Gouge, M.F., Heigel, J.C., Michaleris, P. and Palmer, T.A. (2015), "Modelling forced convection in the thermal simulation of laser cladding process", *The International Journal of Advanced Manufacturing Technology*, Vol. 79 Nos 1/4, pp. 307-320.

Graf, M., Pradjadhiana, K.P., Hälsig, A., Manurung, Y.H.P. and Awiszus, B. (2018), "Numerical simulation of metallic wire arc additive manufacturing (WAAM)", *AIP Conference Proceedings* 19-60.

Groth, C., Kravitz, N.D., Jones, P.E., Graham, J.W. and Redmond, W.R. (2014), "Three-dimensional printing technology", *Journal of Clinical Orthodontics : Jco*, Vol. 48 No. 8, pp. 475-485. https://doi.org/10.5772/60010

Gu, D.D. and Shen, Y.F. (2009), "Balling phenomena in direct laser sintering of stainless-steel powder: metallurgical mechanisms and control methods", *Materials & Design*, Vol. 30 No. 8, pp. 2903-2910.

Guo, N. and Leu, M.C. (2013), "Additive manufacturing: technology, applications and research needs", *Frontiers of Mechanical Engineering*, Vol. 8 No. 3, pp. 215-243.

Gusarov, A.V. and Kruth, J.P. (2005), "Modelling of radiation transfer in metallic powder at laser treatment", *International Journal of Heat and Mass Transfer*, Vol. 48 No. 16, pp. 3423-3434.

Gusarov, A.V., Yadroitsev, I., Bertrand, P. and Smurov, I. (2009), "Model of radiation and heat transfer in laser powder interaction zone at selective laser melting", *Journal of Heat Transfer*, Vol. 131 No. 7, Article No. – 072101.

Hadadzadeh, A., Baxter, C., Amirkhiz, B.S. and Mohammadi, M. (2018), "Strengthening mechanisms in direct metal laser sintered AlSi10Mg: comparison between virgin and recycled powder", *Additive Manufacturing*, Vol. 23, pp. 108-120.

Haeri, S., Wang, Y., Ghita, O. and Sun, J. (2017), "Discrete element simulation and experimental study of powder spreading process in additive manufacturing", *Powder Technology*, Vol. 306, pp. 45-54.

Hänninen, J. (2001), "DMLS moves from rapid tooling to rapid manufacturing", *Metal Powder Report*, Vol. 56 No. 9, pp. 24-29.

He, X., Debroy, T. and Fuerschbach, P.W. (2003), "Probing temperature during laser spot welding from vapour composition and modelling", *Journal of Applied Physics*, Vol. 94 No. 10, pp. 6949-6958.

He, X., Debroy, T. and Fuerschbach, P.W. (2004), "Composition change of stainless steel during micro-joining with short laser pulse", *Journal of Applied Physics*, Vol. 96 No. 8, pp. 4547-4555.

Heigel, J.C., Michaleris, P. and Palmer, T.A. (2015), "Measurement of forced surface convection in directed energy deposition additive manufacturing", *Journal of Engineering Manufacture*, Vol. 230 No. 7, pp. 1295-1308.

Heigemann, L., Agarwal, Weddeling, C. and Tekkaya, A.E. (2016), "Reducing the stair step effect of layer manufactured surface by ball burnishing", Proceedings of the 19th International ESAFORM Conference on Material Forming, AIP conference proceedings 1769(1), pp. 1-6, 190002.

Henwood, C., Bibby, M., Goldak, J. and Watt, D.F. (1988), "Coupled transient heat transfer – microstructure weld computations, (part b)", *ACTA Metallurgica*, Vol. 36 No. 11, pp. 3037-3046.

Herbold, E.B. Walton, O. and Homel, M.A. (2015), "Simulation of powder layer deposition in additive manufacturing processes using the discrete element method", United States: N. P. Web, available at: https://doi.org/10.2172/1239200

Hibbitt, H.D. and Marcal, P.V. (1973), "A numerical, thermo-mechanical model for the welding and subsequent loading of the fabricated structure", *Computers & Structures*, Vol. 3 No. 5, pp. 1145-1174.

Hodge, N. Ferencz, R. and Solberg, J. (2013), "Implementation of a thermomechanical model in diablo for the simulation of selective laser melting", Report, Lawrence Livermore National Laboratory, Livermore, available att: https://doi.org/10.2172/1108835

Hofmeister, W., Wert, M., Smugeresky, J., Philliber, J.A., Griffith, M. and Ensz, M. (1999), "Investigating solidification with the laser-engineered net shaping (LENS) process", *The Member Journal of the Minerals, Metals, & Material Society*, Vol. 51 No. 7, available at: www.tms.org/pubs/journals/JOM/9907/Hofmeister/Hofmeister-9907.html

Hui, D., Goodridge, R.D., Scotchford, C.A. and Grant, D.M. (2018), "Laser sintering of nano-hydroxyapatite coated polyamide 12 powders", *Additive Manufacturing*, Vol. 22, pp. 560-570.

Hussein, A., Hao, L., Yan, C. and Everson, R. (2013), "Finite element simulation of the temperature and stress fields in single layers built without-support in selective laser melting", *Materials & Design (1980-2015)*, Vol. 52, pp. 638-647.

Ingole, D.S., Kuthe, A.M., Thakare, S.B. and Talankar, A.T. (2009), "Rapid prototyping – a technology transfer approach for development of rapid tooling", *Rapid Prototyping Journal*, Vol. 15 No. 4, pp. 280-290.

Ivanova, O., Williams, C. and Campbell, T. (2013), "Additive manufacturing (AM) and nanotechnology: promises and challenges", *Rapid Prototyping Journal*, Vol. 19 No. 5, pp. 353-364.

Jay, O., Toyserkani, E., Donnadieu, P., Blandin, J.J. and Esmaeili, S. (2018), "Selective laser assisted deposition of silver nanoparticles on a Mg-2Wt.% Ca substrate", *Journal of Physics D: Applied Physics*, Vol. 51 Article No. 315401.

Jeng, J.Y., Peng, S.C. and Chou, C.J. (2000), "Metal rapid prototype fabrication using selective laser cladding technology", *The International Journal of Advanced Manufacturing Technology*, Vol. 16 No. 9, pp. 681-687.

Jia, Q. and Gu, D. (2014), "Selective laser melting additive manufacturing of inconel 718 superalloy parts: densification, microstructure and properties", *Journal of Alloys and Compounds*, Vol. 585, pp. 713-721.

Jiang, W., Dalgarno, K.W. and Childs, T.H.C. (2002), "Finite element analysis of residual stresses and deformation in direct metal SLS process", *Proceedings of the 13th Annual International Solid Freeform Fabrication Symposium – An Additive Manufacturing Conference, Solid Freeform Fabrication* pp. 340-348, available at: https://sffsymposium.engr.utexas.edu/Manuscripts/2002/2002-38-Jiang.pdf

Johanson, J.R. (2016), "A rolling theory of granular solids", *Journal of Applied Mechanics*, Vol. 32 No. 4, pp. 842-848.

Jullien, R. and Meakin, P. (1987), "Simple three-dimensional models for ballistic deposition with restructuring", *EPL (Europhysics Letters)*, Vol. 4 No. 12, available at: https://doi.org/10.1209/0295-5075/4/12/008

Kamara, A.M., Marimuthu, S. and Li, L. (2011), "A numerical investigation into residual stress characteristics in laser deposited multiple layer waspaloy parts", *Journal of Manufacturing Science and Engineering*, Vol. 133 No. 3, Article No. 031013.

Karapatis, N.P., Egger, G., Gygax, P.E. and Glardon, R. (1999), "Optimization of powder layer density in selective laser sintering", *10th Annual International Solid Freeform Fabrication Symposium* pp. 255-263, available at: https://sffsymposium.engr.utexas.edu/Manuscripts/1999/1999-029-Karapatis.pdf

Karlsson, R.I. and Josefson, B.L. (1990), "Three-dimensional finite element analysis of temperatures and stresses in a single pass butt welded joint", *Journal of Pressure Vessel Technology*, Vol. 112 No. 1, pp. 76-84.

Keller, N. and Ploshikhin, V. (2014), "New method for fast predictions of residual stress and distortion in AM parts", *25th Annual International Solid Freeform Fabrication Symposium* pp. 1229-1237, available at: http://sffsymposium.engr.utexas.edu/sites/default/files/2014-096-Keller.pdf

Kempen, K., Thijs, L., Vrancken, B., Buls, S., Humbeeck, J.V. and Kruth, J.P. (2013), "Producing crack free, high density M2 HSS parts by selective laser melting: pre heating the base plate", *24th Annual International Solid Freeform Fabrication Symposium* pp. 131-139, available at: https://sffsymposium.engr.utexas.edu/Manuscripts/2013/2013-10-Kempen.pdf

Khairallah, S. and Anderson, A. (2014), "Mesoscopic simulation model of selective laser melting of stainless-steel powder", *Journal of Materials Processing Technology*, Vol. 214 No. 11, pp. 2627-2636.

Klingbeil, N.W., Zinn, J.W. and Beuth, J.L. (1997), "Measurement of residual stress in parts created by shape metal deposition", *8th Annual International Solid Freeform Fabrication Symposium* pp. 125-132, available at: https://sffsymposium.engr.utexas.edu/Manuscripts/1997/1997-14-Klingeil.pdf

Klingbeil, N.W., Beuth, J.L., Chin, R.K. and Amon, C.H. (1998), "Measurement and modelling of residual Stress-Induced warping in direct metal deposition processes", *9th Annual International Solid Freeform Fabrication Symposium, University of TX* pp. 367-374, available at: https://sffsymposium.engr.utexas.edu/Manuscripts/1998/1998-40-Klingbeil.pdf

Körner, C., Attar, E. and Heinl, P. (2011), "Mesoscopic simulation of selective beam melting processes", *Journal of Materials Processing Technology*, Vol. 211 No. 6, pp. 978-987.

Kouhi, M., Fathi, M., Venugopal, J.R., Shamanian, M. and Ramakrishna, S. (2017), "Preparation and characterization of bio-hybrid poly (3-hydroxybutyrate-co-3-hydroxyvalerate) based nano-fibrous scaffolds", *6th International Biennial Conference on ultrafine grained and nanostructured materials: UFGNSM* Kish Island.

Krol, T.A., Seidel, C., Schilp, J., Hofmann, M., Gan, W. and Zaeh, M.F. (2013), "Verification of structural simulation results of metal-based additive manufacturing by means of neutron diffraction", *Physics Procedia*, Vol. 41, pp. 849-857.

Kroos, J., Gratzke, U., Vicanek, M. and Simon, G. (1993), "Dynamic behaviour of the keyhole in laser welding", *Journal of Physics D: Applied Physics*, Vol. 26 No. 3, pp. 481-486.

Kruth, J.P., Leu, M.C. and Nakagawa, T. (1998), "Progress in additive manufacturing and rapid prototyping", *CIRP Annals*, Vol. 47 No. 2, pp. 525-540.

Kruth, J.P., Froyen, L., Vaerenbergh, J.V., Mercelis, P., Rombouts, M. and Lauwers, B. (2004), "Selective laser melting of iron-based powder", *Journal of Materials Processing Technology*, Vol. 149 Nos 1/3, pp. 616-622.

Kula, E. and Weiss, V. (1982), "Residual stress and stress relaxation", *Sagamore Army Materials Research Conference Proceedings*, 28, Springer-Verlag, available at: https://doi.org/10.1007/978-1-4899-1884-0

La Batut, B., De, Fergani, O., Brotan, V., Bambach, M., Mansouri, M. and El, (2017), "Analytical and numerical temperature prediction in direct metal deposition of Ti6Al4V", *Journal of Manufacturing and Materials Processing*, Vol. 1 No. 1, pp. 1-14.

Lange, F.F., Lam, D.C.C. and Sudre, O. (1989), "Powder processing and densification of ceramic composites", *Symposium L – Processing Science of Advanced Ceramics* 155, pp. 309-318, available at: https://doi.org/10.1557/PROC-155-309

Le, H.P. (1998), "Progress and trends in ink-jet printing technology", *Journal of Imaging Science and Technology*, Vol. 42 No. 1, pp. 49-62, available at: www.imaging.org/site/PDFS/Papers/1999/RP-0-92/1975.pdf

Leblond, J.B. and Devaux, J. (1984), "A new kinetic model for an-isothermal metallurgical transformations in steel including effect of austenite grain size", *ACTA Metallurgica*, Vol. 32 No. 1, pp. 137-146.

Leigh, S.J., Bradley, R.J., Purssell, C.P., Billson, D.R. and Hutchins, D.A. (2012), "A simple, Low-Cost conductive composite material for 3D printing of electronic sensors", *PLoS One*, Vol. 7 No. 11, pp. e49365.

Li, Y. and Gu, D. (2014), "Parametric analysis of thermal behaviour during selective laser melting additive manufacturing of aluminium alloy powder", *Materials & Design*, Vol. 63, pp. 856-867.

Li, C., Fu, C.H., Guo, Y.B. and Fang, F.Z. (2016), "A multiscale modelling approach for fast prediction of part distortion in selective laser melting", *Journal of Materials Processing Technology*, Vol. 229, pp. 703-712.

Li, C., Guo, Y., Fang, X. and Fang, F. (2018b), "A scalable predictive model and validation for residual stress and distortion in selective laser melting", *CIRP Annals – Annals*, Vol. 67 No. 1, pp. 249-252.

Li, C., Liu, Z.Y., Fang, X.Y. and Guo, Y.B. (2018a), "Residual stress in metal additive manufacturing", *Procedia Cirp*, Vol. 71, pp. 348-353.

Li, C., Liu, J.F., Fang, X.Y. and Guo, Y.B. (2017), "Efficient predictive model of part distortion and residual stress in selective laser melting", *Additive Manufacturing*, Vol. 17, pp. 157-168.

Li, Y., Zhou, K., Tan, P., Tor, S.B., Chua, C.K. and Leong, K. F. (2018c), "Modelling temperature and residual stress fields in selective laser melting", *International Journal of Mechanical Sciences*, Vol. 136, pp. 24-35.

Lindgren, L.E. and Hedblom, E. (2001), "Modelling of addition of filler material in large deformation analysis of multi-pass welding", *Communications in Numerical Methods in Engineering*, Vol. 17 No. 9, pp. 647-657.

Liu, Y., Yang, Y. and Wang, D. (2016), "A study on the residual stress during selective laser melting (SLM) of metallic powder", *The International Journal of Advanced Manufacturing Technology*, Vol. 87 No. 1-4, pp. 647-656.

Liu, F.R., Zhang, Q., Zhou, W.P., Zhao, J.J. and Chen, J.M. (2012), "Micro scale 3D FEM simulation on thermal evolution within the porous structure in selective laser sintering", *Journal of Materials Processing Technology*, Vol. 212 No. 10, pp. 2058-2065.

Liu, S., Yuen, M., White, E.L., Boley, J.W., Deng, B., Cheng, G.J. and Bottiglio, R.K. (2018), "Laser sintering of liquid nanoparticles for scalable manufacturing of soft and flexible electronics", *ACS Applied Materials and Interfaces*, available at: https://doi.org/10.1021/acsami.8b08722

Löber, L., Schimansky, F.P., Kühn, U., Pyczak, F. and Eckert, J. (2014), "Selective laser melting of a beta solidifying TNM-B1 titanium aluminide alloy", *Journal of Materials Processing Technology*, Vol. 214 No. 9, pp. 1852-1860.

Long, T., Zhang, X., Huang, Q., Liu, L., Liu, Y. and Ren, J. (2018), "Novel Mg-based alloys by selective laser melting for biomedical application microstructure evolution, micro-hardness and in-vitro degradation behaviour", *Virtual and Physical Prototyping*, Vol. 13 No. 2, pp. 71-81.

Lu, J. (1996), *Handbook of Measurement of Residual Stresses*, The Fairmont Press Lilburn, GA, available at: www.prenhall.com/books/ptr_013255738X.html

Lu, L.X., Sridhar, N. and Zhang, Y.W. (2017), "Phase field simulation of powder bed based additive manufacturing", *Acta Materialia*, Vol. 144, pp. 801-809.

Luo, Z. and Zhao, Y. (2018), "A survey of finite element analysis of temperature and thermal stress fields in powder bed fusion additive manufacturing", *Additive Manufacturing*, Vol. 21, pp. 318-332.

Ma, L. and Bin, H. (2007), "Temperature and stress analysis and simulation in fractal scanning-based laser sintering", *The International Journal of Advanced Manufacturing Technology*, Vol. 34 No. 9-10, pp. 898-903.

Mainprize, J.G., Carton, A.K., Klausz, R., Li, Z., Hunter, D. H., Mawdsley, D.W., Muller, S. and Yaffe, M.J. (2018), "Development of a physical 3D anthropomorphic breast texture model using selective laser sintering rapid prototype printing", *Proceedings SPIE 10573, Medical Imaging: Physics of Medical Imaging*, TX.

Markl, M. and Körner, C. (2016), "Multiscale modelling of powder bed based additive manufacturing", *Annual Review of Material Research*, Vol. 46, pp. 15.1-15.31, available at: https://doi.org/10.1146/annurev-matsci-070115-032158

Markl, M. and Körner, C. (2018), "Powder layer deposition algorithm for additive manufacturing simulations", *Powder Technology*, Vol. 330, pp. 125-136.

Mashubuchi, K. (1980), *Analysis of Welded Structure: residual Stress, Distortion and Their Consequences*, Pergamon Press, NewYork, available at: https://doi.org/10.1016/B978-0-08-022714-6.50010-1

Masoomi, M., Thompson, S.M. and Shamsaei, N. (2017), "Laser powder bed fusion of Ti-6Al-4V parts: thermal modelling and mechanical implications", *International Journal of Machine Tools and Manufacture*, Vol. 118–119, pp. 73-90.

Masubuchi, K. (1970), "Control of distortion and shrinkage in welding", Welding Research Council Bulletin No. 149, available at: https://trid.trb.org/view/108610

Masubuchi, K. (1980), *Analysis of Welded Structure: Residual Stresses, Distortion and Their Consequences*, Pergamon Press, New York, NY available at: https://lib.ugent.be/catalog/rug01:001997958

Matsumoto, M., Shiomi, M., Osakada, K. and Abe, F. (2002), "Finite element analysis of single layer forming on metallic powder bed in rapid prototyping by selective laser processing", *International Journal of Machine Tools and Manufacture*, Vol. 42 No. 1, pp. 61-67.

Matthews, M.J., Guss, G., Khairallah, S.A., Rubenchik, A.M., Depond, P.J. and King, W.E. (2016), "Denudation of metal powder layers in laser powder bed fusion process", *Acta Materialia*, Vol. 114, pp. 33-42.

Meakin, P. and Jullien, R. (1987), "Restructuring effects in the rain model for random deposition", *Journal de Physique*, Vol. 48 No. 10, pp. 1651-1662.

Mercelis, P. and Kruth, J.P. (2006), "Residual stresses in selective laser sintering and selective laser melting", *Rapid Prototyping Journal*, Vol. 12 No. 5, pp. 254-265.

Meteyer, S., Xu, X., Perry, N. and Zhao, Y.F. (2014), "Energy and material flow analysis of binder-jetting additive manufacturing processes", *Procedia Cirp*, Vol. 15, pp. 19-25.

Michaleris, P. (2014), "Modelling metal deposition in heat transfer analyses of additive manufacturing process", *Finite Elements in Analysis and Design*, Vol. 86, pp. 51-60.

Michaleris, P. and De-Biccari, A. (1997), "Prediction of welding distortion", *Welding Journal*, Vol. 76 No. 4, pp. 172-180, available at: https://canteach.candu.org/Content%20Library/20053410.pdf

Michaleris, P. and Sun, X. (1997), "Finite element analysis of thermal tensioning techniques mitigating weld buckling distortion", *Welding Journal*, Vol. 76 No. 11, pp. 451s-457s available at: http://files.aws.org/wj/supplement/WJ_1997_11_s451.pdf

Michaleris, P., Dantzig, J. and Tortorelli, D. (1999), "Minimization of welding residual stress and distortion in large structures", *Welding Journal*, Vol. 78 No. 11, pp. 361s-366s available at: http://files.aws.org/wj/supplement/WJ_1999_11_s361.pdf

Michaleris, P., Zhang, L., Bhide, S.R. and Marugabandhu, P. (2006), "Evaluation of 2D, 3D and applied plastic strain methods for predicting buckling welding distortion and residual stress", *Science and Technology of Welding and Joining*, Vol. 11 No. 6, pp. 707-716, available at: https://doi.org/10.1179/174329306X147724

Mindt, H.W., Megahed, M., Lavery, N.P., Holmes, M.A. and Brown, S.G.R. (2016), "Powder bed layer characteristics: the overseen first order process input", *Metallurgical and Materials Transactions A*, Vol. 47 No. 8, pp. 3811-3822.

Mukherjee, T., Manvatkar, V.A. and Debroy, T. (2017a), "Mitigation of thermal distortion during additive manufacturing", *Scripta Materialia*, Vol. 127, pp. 79-83.

Mukherjee, T., Zhang, W. and Debroy, T. (2017b), "An improved prediction of residual stresses and distortion in additive manufacturing", *Computational Materials Science*, Vol. 126, pp. 360-372.

Mukherjee, T., Zuback, J.S., De, A. and DebRoy, T. (2016), "Printability of alloys for additive manufacturing", *Scientific Reports – Reports*, Vol. 6.

Mukherjee, T., Zuback, J.S., Zhang, W. and DebRoy, T. (2018), "Residual stress and distortion in additively manufactured compositionally graded and dissimilar joints", *Computational Materials Science*, Vol. 143, pp. 325-337.

Nelson, J.C., Xue, S., Barlow, J.W., Beaman, J.J., Marcus, H. L. and Bourell, D.L. (1993), "Model of the selective laser sintering of bisphenol-A polycarbonate", *Industrial & Engineering Chemistry Research*, Vol. 32 No. 10, pp. 2305-2317.

Nickel, A.H., Barnett, D.M. and Prinz, F.B. (2001), "Thermal stresses and deposition pattern in layered manufacturing", *Materials Science and Engineering: A*, Vol. 317 Nos 1/2, pp. 59-64.

Nickel, A., Barnett, D., Link, G. and Prinz, F. (1999), ""Residual stresses in layered manufacturing", *Proceedings of the 10th Annual International Solid Freeform Fabrication Symposium – An Additive Manufacturing Conference, Solid Freeform Fabrication*, pp. 239-246, available at: https://sffsymposium.engr.utexas.edu/Manuscripts/1999/1999-027-Nickel.pdf

Ning, F., Hu, Y., Liu, Z., Wang, X., Li, Y. and Cong, W. (2018), "Ultrasonic vibration assisted laser engineered net shaping of inconel 718 parts: microstructural and mechanical characterization", *Journal of Manufacturing Science and Engineering*, Vol. 140 No. 6, Article No. MANU-17-1439.

Niu, H.J. and Chang, I.T.H. (1999), "Instability of scan tracks of selective laser sintering of high-speed steel powder", *Scripta Materialia*, Vol. 41 No. 11, pp. 1229-1234.

Ocelik, V., Bosgra, J. and de Hosson, J.T.M. (2009), "In-situ strain observation in high power laser cladding", *Surface and Coatings Technology*, Vol. 203 Nos 20/21, pp. 3189-3196.

Ogino, Y., Asai, S. and Hirata, Y. (2018), "Numerical simulation of WAAM process by a GMAW weld Pool model", *Welding in the World*, Vol. 62 No. 2, pp. 393-401.

Onuike, B., Heer, B. and Bandyopadhyay, A. (2018), "Additive manufacturing of inconel 718 – copper alloy bimetallic structure using laser engineered net shaping", *Additive Manufacturing*, Vol. 21, pp. 133-140.

Optomec (2020), "The technology behind LENS", available at: www.optomec.com/3d-printed-metals/lens-technology/

Papadakis, L., Branner, G., Schober, A., Richter, K.-H. and Uihlein, T. (2012), "Numerical modelling of heat effects during thermal manufacturing of aero engine components", *Proceedings of World Congress on Engineering*, 4-6 July, London, available at: www.iaeng.org/publication/WCE2012/WCE2012_pp1518-1523.pdf

Papadakis, L., Loizou, A., Risse, J., Bremen, S. and Schrage, J. (2014), "A computational reduction model for appraising structural effects in selective laser melting manufacturing", *Virtual and Physical Prototyping*, Vol. 9 No. 1, pp. 17-25.

Papazoglou, V.J. and Masubuchi, K. (1982), "Numerical analysis of thermal stresses during welding including phase transformation effects", *Journal of Pressure Vessel Technology*, Vol. 140 No. 3, pp. 198-203.

Parry, L., Ashcroft, I.A. and Wildman, R.D. (2016), "Understanding the effect of laser scan strategy on residual stress in selective laser melting through thermo-mechanical simulation", *Additive Manufacturing*, Vol. 12, pp. 1-15.

Parteli, E.J.R. and Pöschel, T. (2016), "Particle based simulation of powder application in additive manufacturing", *Powder Technology*, Vol. 288, pp. 96-102.

Patil, R.B. and Yadava, V. (2007), "Finite element analysis of temperature distribution in single metallic powder layer during metal laser sintering", *International Journal of Machine Tools and Manufacture*, Vol. 47 Nos 7/8, pp. 1069-1080.

Perez, K.B. and Williams, C.B. (2013), "Combining additive manufacturing and direct write for integrated electronics – a review", *24th Annual International Solid Freeform Fabrication Symposium* University of TX, Austin, pp. 962-979, available at: http://sffsymposium.engr.utexas.edu/Manuscripts/2013/2013-77-Perez.pdf

Peyre, P., Aubry, P., Fabbro, R., Neveu, R. and Longuet, A. (2008), "Analytical and numerical modelling of the direct metal deposition laser process", *Journal of Physics D: Applied Physics*, Vol. 41 025403-1–025403-10.

Pham, D.T. and Dimov, S.S. (2001), *Rapid Manufacturing*, Springer-Verlag, London, available at: https://doi.org/10.1007/978-1-4471-0703-3

Pham, D.T. and Gault, R.S. (1998), "A comparison of rapid prototyping technologies", *International Journal of Machine Tools and Manufacture*, Vol. 38 No. 10 – 11, pp. 1257-1287.

Raabe, D. (2002), "Cellular automata in material science with particular reference to recrystallization simulation", *Annual Review of Materials Research*, Vol. 32 No. 1, pp. 53-76.

Raghavan, A., Wei, H.L., Palmer, T.A. and Debroy, T. (2013), "Heat transfer and fluid flow in additive manufacturing", *Journal of Laser Applications*, Vol. 25 No. 5, 052006-1–052006-8.

Rahmati, S. and Vahabli, E. (2015), "Evaluation of analytical modelling for improvement of surface roughness of FDM test part using measurement results", *The International Journal of Advanced Manufacturing Technology*, Vol. 79 Nos 5/8, pp. 823-829.

Rai, A., Markl, M. and Körner, C. (2016), "A coupled cellular automaton – lattice Boltzmann model for grain structure simulation during additive manufacturing", *Computational Materials Science*, Vol. 124, pp. 37-48.

Raju, M., Gupta, M.K., Bhanot, N. and Sharma, V.S. (2018), "A hybrid PSO-BFO evolutionary algorithm for optimization of fused deposition modelling process parameters", *Journal of Intelligent Manufacturing*, Vol. 1, pp. 1-16.

Rappaz, M. and Gandin, C.A. (1993), "Probabilistic modelling of microstructure formation in solidification process", *Acta Metallurgica et Materialia*, Vol. 41 No. 2, pp. 345-360.

Rausch, A.M., Markl, M. and Körner, C. (2018), "Predictive simulation of process windows for powder bed fusion additive manufacturing: influence of the powder size distribution", *Computers & Mathematics with Applications*, Vol. 11.

Ren, J., Liu, J. and Yin, J. (2010), "Simulation of transient temperature field in the selective laser sintering process of W/Ni powder mixture", *International Conference on Computer and Computing Technologies in Agriculture*, Vol. 347, pp. 494-503, Springer, Berlin, Heidelberg, available at: https://doi.org/10.1007/978-3-642-18369-0_59

Riedlbauer, D., Steinmann, P. and Mergheim, J. (2014), "Thermomechanical finite element simulations of selective electron beam melting processes: performance considerations", *Computational Mechanics*, Vol. 54 No. 1, pp. 109-122.

Roberts, I.A., Wang, C.J., Esterlein, R., Stanford, M. and Mynors, D.J. (2009), "A three-dimensional finite element analysis of the temperature field during laser melting of metal powders in additive later manufacturing", *International Journal of Machine Tools and Manufacture*, Vol. 49 Nos 12/13, pp. 916-923.

Rowe, J. (2018), "Wohlers report 2018: am grows overall with metal rising", available at: www10.mcadcafe.com/blogs/jeffrowe/2018/05/03/wohlers-report-2018-am-grows-overall-with-metal-rising/ (accessed 08 July 2019)

Rubenchik, A.S., Wu, S., Mitchell, S., Golosker, I., LeBlanc, M. and Peterson, N. (2015), "Direct measurements of temperature dependent laser absorptivity of metal powders", *Applied Optics*, Vol. 54 No. 24, pp. 7230-7233.

Sachdeva, A., Singh, S. and Sharma, V.S. (2013), "Investigating surface roughness of parts produced by SLS process", *The International Journal of Advanced Manufacturing Technology*, Vol. 64 No. 9-12, pp. 1505-1516.

Sachs, E., Cima, M. and Cornie, J. (1990), "Three-dimensional printing: rapid tooling and prototypes directly from CAD model", *CIRP Annals*, Vol. 39 No. 1, pp. 201-204.

Sahoo, S. and Chou, K. (2015), "Phase-field simulation of microstructure evolution of Ti-6Al-4V in electron beam additive manufacturing process", *Additive Manufacturing*, Vol. 9, pp. 14-24.

Sames, W.J., Medina, F., Peter, W., Babu, S. and Dehoff, R. (2014), "Effect of process control and powder quality on inconel 718 produced using electron beam melting", *Proceedings of the 8th International Symposium on Super-alloy 718 and Derivatives* pp. 409-423, available at: https://doi.org/10.1002/9781119016854.ch32

Schilp, J., Seidel, C., Krauss, H. and Weirather, J. (2014), "Investigation on temperature fields during laser beam melting by means of process monitoring and multiscale process modelling", *Advances in Mechanical Engineering*, Vol. 6 Article No. 217584,

Schoinochoritis, B., Chantzis, D. and Salonitis, K. (2014), "Simulation of metallic powder bed additive manufacturing processes with the finite element method: a critical review", *Journal of Engineering Manufacture*, Vol. 231 No. 1, pp. 96-117.

Sealy, M.P., Madireddy, G., Williams, R.E., Rao, P. and Toursangsaraki, M. (2018), "Hybrid processes in additive manufacturing", *Journal of Manufacturing Science and Engineering*, Vol. 140 No. 6, Article No. MANU-17-1429.

Shanjani, Y. and Toyserkani, E. (2008), ""Material spreading and compaction in powder based solid free-form fabrication methods: mathematical modelling", *19th Annual International Solid Freeform Fabrication Symposium* pp. 399-410, available at: http://edge.rit.edu/edge/P10551/public/SFF/SFF%202008%20Proceedings/Manuscripts/2008-36-Shanjani.pdf

Sharma, V.S., Singh, S., Sachdeva, A. and Kumar, P. (2015), "Influence of sintering parameters on dynamic mechanical properties of selective laser sintered parts", *International Journal of Material Forming*, Vol. 8 No. 1, pp. 157-166.

Shellabear, M. and Nyrhila, O. (2004), "DMLS-development history and state of the art", *4th Laser assisted net shape engineering proceedings (LANE)*, Erlangen, pp. 21-24, available at: www.i3dmfg.com/wp-content/uploads/2015/07/History-of-DMLS.pdf

Shen, N. and Chou, K. (2012), "Thermal modelling of electron beam additive manufacturing process – powder sintering effect", *Proceedings of the ASME International Manufacturing Science and Engineering Conference* pp. 287-295.

Shishkovsky, I., Morozov, Y. and Smurov, I. (2007), "Nano-fractal surface structure under laser sintering of titanium and nitinol for bone tissue engineering", *Applied Surface Science*, Vol. 254 No. 4, pp. 1145-1149.

Sih, S.S. and Barlow, J.W. (1994), "Measurement and prediction of the thermal conductivity of powders at high temperature", *Proceedings of the 5th Annual International Solid Freeform Fabrication* Symposium – An Additive Manufacturing Conference, Solid Freeform Fabrication pp. 321-329, available at: https://sffsymposium.engr.utexas.edu/Manuscripts/1994/1994-35-Sih.pdf

Sih, S.S. and Barlow, J.W. (1995), "The prediction of the thermal conductivity of the powders", *Proceedings of the 6th Annual International Solid Freeform Fabrication* Symposium – An Additive Manufacturing Conference, Solid Freeform Fabrication pp. 397 - 401, available at: https://sffsymposium.engr.utexas.edu/Manuscripts/1995/1995-49-Sih.pdf

Sih, S.S. and Barlow, J.W. (2004), "The prediction of emissivity and thermal conductivity of powder beds", *Particulate Science and Technology*, Vol. 22 No. 4, pp. 291-304.

Singh, S., Sharma, V.S. and Sachdeva, A. (2012), "Optimization and analysis of shrinkage in selective laser sintered polyamide parts", *Materials and Manufacturing Processes*, Vol. 27 No. 6, pp. 707-714.

Singh, S., Sharma, V.S., Sachdeva, A. and Sinha, S.K. (2013), "Optimization and analysis of mechanical properties for selective laser sintered polyamide parts", *Materials and Manufacturing Processes*, Vol. 28 No. 2, pp. 163-172.

Sirringhaus, H., Kawase, T., Friend, R.H., Shimoda, T., Inbasekaran, M. and Wu, W. (2000), "High-resolution inkjet printing of all-polymer transistor circuits", *Science*, Vol. 290 No. 5499, pp. 2123-2126.

Slotwinski, J.A., Garboczi, E.J., Stutzman, P.E., Ferraris, C.F., Watson, S.S. and Peltz, M.A. (2014), "Characterization of metal powders used for additive manufacturing", *Journal of the Research of the National Institute of Standards and Technology*, Vol. 119, pp. 460-493, Available at: http://dx.doi.org/10.6028/jres.119.018

Soares, O.D.D. and Perez-Amor, M. (1987), "Applied laser tooling", in Soares, O D D. and Perez-Amor, M. (Eds), *Applied Laser Tooling*, Martinus Nijhoff, Dordrecht Available at: https://doi.org/10.1007/978-94-009-3569-3

Srivatsan, T.S. and Sudarshan, T.S. (2016), "Additive manufacturing: Innovations", *Advances and Applications*, CRC Press, Taylor and Francis Group, London.

Srolovitz, D.J., Anderson, M.P., Sahni, P.S. and Grest, G.S. (1684), "Computer simulation of grain growth – II. Grain size distribution, topology, and local dynamics", *Acta Metallurgica*, Vol. 32 No. 5, pp. 793-802.

Stavropoulos, P. and Foteinopoulos, P. (2018), "Modelling of additive manufacturing processes: a review and classification", *Manufacturing Review*, Vol. 5 No. 2.

Strano, G., Hao, L., Everson, R.M. and Evans, K.E. (2012), "Surface roughness analysis, modelling and prediction in selective laser melting", *Journal of Materials Processing Technology*, Vol. 213 No. 4, pp. 589-597.

Stratasysdirect (2018), "Direct metal laser sintering materials", available at: www.stratasysdirect.com/materials/direct-metal-laser-sintering (accessed 31 March 2018).

Sufiiarov, V.S.H., Popovish, A.A., Borisov, E.V., Polozov, I.A., Masaylo, D.V. and Orlov, A.V. (2017), "The effect of layer thickness at selective laser melting", *Procedia Engineering*, Vol. 174, pp. 126-134.

Sutton, A.T., Kriewall, C.S., Leu, M.C. and Newkirk, J.W. (2016), "Powders for additive manufacturing processes: characterization techniques and effect of part properties", *27th Annual International Solid Freeform Fabrication Symposium – An Additive Manufacturing Conference, Solid Freeform Fabrication* pp. 1004-1030, available at: https://pdfs.semanticscholar.org/ec08/10346edcce2d5cac092d3d24835442405d14.pdf

Syvänen, T., Heugel, M. and Domröse, R. (2005), "Diode pumped fibre laser in direct metal laser sintering (DMLS) process", *Laser Materials Processing Conference and Laser Microfabrication Conference, ICALEO, International Congress on Applications of Lasers & Electro-Optics* 97. available at:

www.tib.eu/en/search/id/tema%3ATEMA20050801811/Diode-pumped-fiber-laser-in-direct-metal-laser/

Szost, B.A., Terzi, S., Filomeno, M., Boisselier, D., Prytuliak, A., Pirling, T., Hofmann, M. and Jarvis, D.J. (2016), "A comparative study of additive manufacturing techniques: residual stress and microstructural analysis of CLAD and WAAM printed Ti-6Al-4V components", *Materials & Design*, Vol. 89, pp. 559-567.

Taylor, G.A., Hughes, M., Strusevich, N. and Pericleous, K. (2002), "Finite volume methods applied to the computational modelling of welding phenomena", *Applied Mathematical Modelling*, Vol. 26 No. 2, pp. 311-322.

Tekriwal, P. and Mazumdar, J. (1991), "Transient and residual thermal strain stress analysis of GMAW", *Journal of Engineering Materials and Technology*, Vol. 113 No. 3, pp. 336-343.

Tekriwal, P. and Mazumdar, J. (1988), "Finite element analysis of three dimensional transient heat transfer in GMA welding", *Welding Journal*, pp. 150s-156s, available at: https://app.aws.org/wj/supplement/WJ_1988_07_s150.pdf

Teng, C., Pal, D., Gong, H., Zeng, K., Briggs, K., Patil, N. and Stucker, B. (2017), "A review of defect modelling in laser material processing", *Additive Manufacturing*, Vol. 14, pp. 137-147.

Tiwari, S.K., Pande, S., Bobade, S.M. and Kumar, S. (2018), "A targeted functional value based nanoclay/PA12 composite material development for selectice laser sintering process", *Procedia Manufacturing*, Vol. 21, pp. 630-637.

Tolochko, N.K., Laoui, T., Khlopkov, Y.V., Mozzharou, S.E., Titiv, V.I. and Ignatiev, M.B. (2000), "Absorptance of powder materials suitable for lase sintering", *Rapid Prototyping Journal*, Vol. 6 No. 3, pp. 155-160.

Trapaga, G., Matthys, E.F., Valencia, J.J. and Szekely, J. (1992), "Fluid flow, heat transfer, and solidification of molten metal droplets impinging on substrates: comparison of numerical and experimental results", *Metallurgical Transactions B*, Vol. 23 No. 6, pp. 701-718.

Tripathy, S., Chin, C., London, T., Ankalkhope, U. and Oancea, V. (2017), "Process modelling and validation of powder bed metal additive manufacturing", *NAFEMS World Congress*, Stockholm. available at: www.researchgate.net/publication/319173249_Process_Modeling_and_Validation_of_Powder_Bed_Metal_Additive_Manufacturing

Turner, B.N., Strong, R. and Gold, S.A. (2014), "A review of melt extrusion additive manufacturing processes: I. process design and modelling", *Rapid Prototyping Journal*, Vol. 20 No. 3, pp. 192-204.

Umaras, E. and Tsuzuki, M.S.G. (2017), "Additive manufacturing – consideration on geometric accuracy and factors of influence", *IFAC-PapersOnLine*, Vol. 50 No. 1, pp. 14940-14945.

Usamentiaga, R., Venegas, P., Guerediaga, J., Vega, L., Molleda, J. and Bulnes, F.G. (2014), "Infrared thermography for temperature measurement and non-destructive testing", *Sensors*, Vol. 14 No. 7, pp. 12305-12348.

Vaezi, M., Seitz, H. and Yang, S. (2013), "A review on 3D micro-additive manufacturing technologies", *The International Journal of Advanced Manufacturing Technology*, Vol. 67 Nos 5/8, pp. 1721-1754.

Van Belle, L., Vansteenkiste, G. and Boyer, J.C. (2012), "Comparisons of numerical modelling of the selective laser melting", *Key Engineering Materials*, Vols 504/506, pp. 1067-1072.

Vandenbroucke, B. and Kruth, J. (2007), "Selective laser melting of biocompatible metals for rapid manufacturing of medical parts", *Rapid Prototyping Journal*, Vol. 13 No. 4, pp. 196-203.

Vasinonta, A., Beuth, J. and Griffith, M. (2000), "Process maps for controlling residual stresses and melt Pool size in laser based SFF process", *Proceedings of the 11th Annual International Solid Freeform Fabrication Symposium – An Additive Manufacturing Conference, Solid Freeform Fabrication* pp. 200-208, available at: https://sffsymposium.engr.utexas.edu/Manuscripts/2000/2000-25-Vasinonta.pdf

Vasinonta, A., Beuth, J.L. and Griffith, M. (2007), "Process maps for predicting residual stress and melt Pool size in the Laser-Based fabrication of Thin-Walled structures", *Journal of Manufacturing Science and Engineering*, Vol. 129 No. 1, pp. 101-109.

Vatsola, G., Zhang, G., Pei, Q.X. and Zhang, Y.W. (2016), "Controlling of residual stress in additive manufacturing of Ti6Al4V by finite element modelling", *Additive Manufacturing* , Vol. 12, pp. 231-239.

Venuvinod, P.K. and Ma, W. (2004), *Rapid Prototyping: Laser-Based and Other Technologies*, Springer, London, available at: https://doi.org/10.1007/978-1-4757-6361-4

Vilar, R. (2014), "Laser powder deposition", *Comprehensive Materials Processing* Vol. 10, pp. 163-216, available at: https://doi.org/10.1016/B978-0-08-096532-1.01005-0

Wang, L. and Felicelli, S. (2007), "Process modelling in laser deposition of multilayer SS410 steel", *Journal of Manufacturing Science and Engineering*, Vol. 129 No. 6, pp. 1028-1034.

Wang, Z., Palmer, T.A. and Beese, A.M. (2016), "Effect of processing parameters on microstructure and tensile properties of austenitic stainless steel 304L made by directed energy deposition additive manufacturing", *ACTA Materialia*, Vol. 110, pp. 226-235.

Wang, D.N., Wang, Y., Liao, C.R., (2015), "Femtosecond laser micromachining on optical fibre", in Lawrence, J. and Waugh, D.G. *Laser Surface Engineering – Processes and Applications*, ", Woodhead Publishing Sawston, pp. 359-381, Available at: https://doi.org/10.1016/B978-1-78242-074-3.00014-3

Wang, Z., Denlinger, E.R., Michaleris, P., Stoica, A.D., Ma, D. and Beese, A.M. (2017), "Residual stress mapping in inconel 625 fabricated through additive manufacturing: method for neutron diffraction measurements to validate thermomechanical model predictions", *Materials & Design*, Vol. 113, pp. 169-177.

Watt, D.F., Coon, L., Bibby, M., Goldak, J. and Henwood, C. (1988), "An algorithm for modelling microstructural development in weld heat affected zones (part a) reaction kinetics", *ACTA Metallurgica*, Vol. 36 No. 11, pp. 3029-3035.

Wen, S. and Shin, Y.C. (2010), "Modelling of transport phenomena during the coaxial laser direct deposition process", *Journal of Applied Physics*, Vol. 108 No. 4, Article No. – 044908.

Wheeler, A.A., McFadden, G.B. and Boettinger, W.J. (1996), "Phase-field model for solidification of a eutectic alloy", *Proceedings of the royal society A, Mathematical, Physical and Engineering Sciences* 452, pp. 495-525.available at: https://doi.org/10.1098/rspa.1996.0026

Withers, P.J. and Bhadeshia, H.K.D.H. (2001), "Residual stress, part 2 – nature and origins", *Materials Science and Technology*, Vol. 17 No. 4, pp. 366-375.

Woesz, A. (2010), "Rapid prototyping to produce porous scaffolds with controlled architecture for possible use in bone tissue engineering", in Bidanda, B. and Bartolo, P. (Eds), *Virtual Prototyping and Bio Manufacturing in Medical Applications*, University of Pittsburgh, Pittsburgh, pp. 171-206, available at: https://doi.org/10.1007/978-0-387-68831-2

Wohlers, T.T. (1991), "Make fiction fact fast", *Manufacturing Engineering*, Vol. 106 No. 3, pp. 44-49.

Wohlers, T.T. (2016), "Wohlers report, wohlers associates".

Wohlers Associates (2018), "Wohlers report 2018 shows dramatic rise in metal additive manufacturing and overall industry growth of 21%", 27 March, available at: https://wohlersassociates.com/press74.html

Wohlers, T. and Gornet, T. (2012), "History of additive manufacturing: part of wohlers report 2012", Wohlers Report 2012, Wohlers Associates. available at: www.wohlersassociates.com/history2012.pdf

Wu, J., Wang, L. and An, X. (2017), "Numerical analysis of residual stress evolution of AlSi10Mg manufactured by selective laser melting", *Optik*, Vol. 137, pp. 65-78.

Xiao, B. and Zhang, Y. (2007), "Laser sintering of metal powders on top of sintered layer under multiple-line laser scanning", *Journal of Physics D: Applied Physics*, Vol. 40 No. 21, pp. 6725-6734.

Yadroitsev, I. (2009), *Selective Laser Melting*, LAP Lambert Academic Publications, Saarbrüvken.

Yadroitsev, I. and Yadroitsev, I. (2015), "Evaluation of residual stress in stainless steel 316L and Ti6Al4V samples produced by selective laser melting", *Virtual and Physical Prototyping*, Vol. 10 No. 2, pp. 67-76.

Yadroitsev, I., Bertrand, P. and Smurov, I. (2007), "Parametric analysis of the selective laser melting process", *Applied Surface Science*, Vol. 253 No. 19, pp. 8064-8069.

Yagi, S. and Kunii, D. (2004), "Studies on effective thermal conductivities in packed beds", *AIChE Journal*, Vol. 3 No. 3, pp. 373-381.

Yang, J., Ouyang, H. and Wang, Y. (2010), "Direct metal laser fabrication: machine development and experimental work", *The International Journal of Advanced Manufacturing Technology*, Vol. 46 No. 9-12, pp. 1133-1143.

Yuan, M. and Bourell, D. (2012), "Efforts to reduce part bed thermal gradients during laser sintering processing", *Proceedings of the 22nd Annual International Solid Freeform Fabrication Symposium – An Additive Manufacturing Conference*, pp. 962-974, available at: https://sffsymposium.engr.utexas.edu/Manuscripts/2012/2012-73-Yuan.pdf

Zaeh, M.F. and Branner, G. (2010), "Investigation on residual stress and deformations in selective laser melting", *Production Engineering*, Vol. 4 No. 1, pp. 35-45.

Zaeh, M.F. and Kahnert, M. (2009), "The effect of scanning strategies on electron beam sintering", *Production Engineering*, Vol. 3 No. 3, pp. 217-224.

Zeng, K., Pal, D., Gong, J., Patil, N. and Stucker, B. (2015), "Comparison of 3DSIM thermal modelling of selective laser melting using new dynamic meshing method to ANSYS", *Materials Science and Technology*, Vol. 31 No. 8, pp. 945-956.

Zhang, Y. and Bandyopadhyay, A. (2018), "Direct fabrication of compositionally graded Ti-Al_2O_3 multi-material structures using laser engineered net shaping", *Additive Manufacturing*, Vol. 21, pp. 104-111.

Zhang, L., Michaleris, P. and Marugabandhu, P. (2007), "Evaluation of applied plastic strain methods for welding distortion prediction", *Journal of Manufacturing Science and Engineering*, Vol. 129 No. 6, pp. 1000-1010.

Zhang, J., Liou, F., Seufzer, W. and Taminger, K. (2016), "A coupled finite element cellular automaton model to predict thermal history and grain morphology of Ti-6Al-4V during direct metal deposition (DMD)", *Additive Manufacturing*, Vol. 11, pp. 32-39.

Zhang, K., Wang, S., Liu, W. and Long, R. (2014), "Effect of substrate preheating on the thin-wall part built by laser metal deposition shaping", *Applied Surface Science*, Vol. 317, pp. 839-855.

Zhang, X., Zhou, B., Zeng, Y. and Gu, P. (2002), "Model layout optimization for solid ground curing rapid prototyping process", *Robotics and Computer-Integrated Manufacturing*, Vol. 18 No. 1, pp. 41-51.

Zhou, J., Zhang, Y. and Chen, J.K. (2009), "Numerical simulation of random packing of spherical particles for powder-based additive manufacturing", *Journal of Manufacturing Science and Engineering*, Vol. 131 No. 3.

Zohdi, T.I. (2014), "Additive particle deposition and selective laser processing – a computational manufacturing framework", *Computational Mechanics*, Vol. 54 No. 1, pp. 171-191.

Zok, F., Lange, F.E. and Porter, J.R. (1991), "Packing density of composite powder mixture", *Journal of the American Ceramic Society*, Vol. 74 No. 8, pp. 1880-1885.

Corresponding author

Shekhar Srivastava can be contacted at: shekhars.ip.17@nitj.ac.in